

Review

# Remediation of Heavy Metals and Organic Pollutants in Soil by Biochar: A Comprehensive Review

Weijian Zhang<sup>1,2</sup>, Zaiwang Zhang<sup>3,\*</sup> and Zenghui Diao<sup>1,2,\*</sup> 

<sup>1</sup> Collage of Resources and Environment, Zhongkai University of Agriculture and Engineering, Guangzhou 510225, China; weijianzhang02@163.com

<sup>2</sup> Guangdong Woye Fertilizer Industry Co., Ltd., Yunfu 527200, China

<sup>3</sup> Shandong Key Laboratory of Eco-Environmental Science for the Yellow River Delta, Shandong University of Aeronautics, Binzhou, 256603, China

\* Correspondence: zzwangbz@163.com (Z.Z.); zenghuid86@163.com (Z.D.)

## Abstract

In recent years, soil contamination by heavy metals and organic pollutants has become a serious environmental problem. Biochar is a highly carbonaceous, water-insoluble porous material made from biomass feedstock through a thermochemical conversion process, and it has been widely used in the remediation of various soil pollutants. However, previous reviews on the modification of biochar and the remediation reaction mechanism of heavy metals and organic pollutants by biochar in soil were still not sufficiently comprehensive. Based on the current research status of the remediation of heavy metals and organic pollutants by biochar in soil, this review systematically summarized biomass feedstock types, pyrolysis methods and their applicable scenarios, as well as the modification strategies of biochar, including pore structure modification, surface functional group modification, surface charge modification, and magnetic modification. It also comparatively discussed the adsorption of heavy metals by biochar mainly through electrostatic attraction, ion exchange, complexation/precipitation, cation- $\pi$  interaction, and redox transformation, while the adsorption of organic pollutants via  $\pi$ - $\pi$ /EDA interactions, electrostatic attraction, hydrogen bonding, hydrophobic partitioning, and pore filling were outlined. The review also discussed competitive effects among pollutants during biochar adsorption under co-contamination scenarios, as well as the synergistic interactions between biochar and soil microorganisms or plants. In addition, the review addressed recent progress in field-scale applications of biochar, as well as the current state of research on aging effects, ecological risks, and economic feasibility. Finally, it identifies key research directions that warrant further attention. This review highlighted the mechanistic differences between heavy metal stabilization and organic pollutant removal in soil by biochar, and provided mechanistic insight and guidance for biochar-based soil remediation.

**Keywords:** biochar; modification method; heavy metals; organic pollutants; soil pollution



Received: 21 March 2026

Revised: 28 April 2026

Accepted: 6 May 2026

Published: 12 May 2026

**Copyright:** © 2026 by the authors. Licensee MDPI, Basel, Switzerland. This article is an open access article distributed under the terms and conditions of the [Creative Commons Attribution \(CC BY\) license](https://creativecommons.org/licenses/by/4.0/).

## 1. Introduction

As the industrialization and modernization of human society accelerate, human activities such as mining, metallurgy, electroplating and excessive use of fertilizers lead to the release of heavy metals into the soil [1–3]. Heavy metals typically exhibit high toxicity, high mobility and non-biodegradability, and these heavy metals adversely affect soil ecological functions by suppressing enzyme activities, reducing microbial biomass, and reshaping microbial community composition, which in turn decreases soil fertility and compromises

soil ecosystem stability [4–6]. Moreover, bioavailable heavy metals can be absorbed by crops, thereby threatening ecological balance in farmland, sustainable agricultural development and food safety [7]. Also, these heavy metals can easily transfer and accumulate within the food chain, posing risks of cancer and neurological diseases when ingested by humans [8–10]. It is worth noting that exchangeable heavy metals in soil are the most significant components affecting human health as they have high bioavailability [11]. In Feyisa's study on the risks to human health from vegetables grown in Ethiopian farmland, it was found that lead levels exceeded the World Health Organization guidelines [12]. Excessive cadmium intake leads to kidney dysfunction and bone demineralization [13], but the residual forms of heavy metals in soil are typically stable and pose little harm human health [14]. Moreover, extensive use of pesticides, fossil fuels and dyes leads to the entry of organic pollutants into soil. These organic pollutants possess properties such as high toxicity, bioaccumulation, persistence and long-range migration [15–19]. Various organic pollutants in soil include persistent organic pollutants (POPs) [20], antibiotics [21], and endocrine disruptors [22], which can also enter the soil through human activities and threaten human health and ecological safety. Thus, it is of critical significance to remediate those polluted soils to reduce or eliminate the adverse impacts of the heavy metals and organic pollutants.

To date, various remediation methods have been used for soil contamination caused by heavy metals and organic pollutants, including ultrasound technology, in situ gas thermal remediation, photocatalysis, electrocatalysis, advanced oxidation and microbial treatment [23–29]. These treatment technologies have unique advantages and limitations. For example, ultrasonic remediation technology is environmentally friendly and efficient, but it faces the challenge of reduced effectiveness due to transmission attenuation in soil-water two-phase systems [24]. In situ gas thermal remediation can rapidly and effectively remove organic compounds from soil using high-temperature gas, but high-temperature treatment often disrupts soil properties, posing risks of secondary pollution [23]. Photocatalytic technology is widely studied due to its low energy consumption, absence of secondary pollution and sustainable effects, but soil severely interferes with photon utilization efficiency, making it difficult to effectively remove deep-seated pollutants [26]. Electrochemical advanced oxidation processes can repair soil by directly generating oxidizing substances at the anode without adding chemical reagents, but their indirect oxidation efficiency is low, and direct oxidation leads to anode contamination in soil [30]. Microbial treatment technologies are environmentally friendly but have the drawbacks of slow efficiency and prolonged remediation time. Therefore, exploring efficient and sustainable environmental remediation strategies has become urgent in the field of soil pollutants [31–33]. Adsorption methods have garnered significant attention due to their advantages of simple operation, low cost, high removal efficiency and broad applicability. Various adsorbent materials like biochar, activated carbon and nanomaterials with high specific surface areas, porous structures and specific properties are used for the effective removal of pollutants [34,35]. Among these, biochar, as an emerging adsorbent, has been widely applied in the remediation of heavy metals and organic pollutants due to its excellent adsorption performance, low cost and ability to enhance soil fertility [36,37]. Actually, biochar is a carbon-rich porous material produced from biomass through thermochemical conversion under oxygen-limited conditions [29,38], which has been widely investigated as an environmentally friendly and low-cost remediation agent for contaminated soils owing to its ability to immobilize heavy metals via adsorption-related interactions, ion exchange, complexation/precipitation, and redox processes. Organic pollutants are absorbed through  $\pi$ - $\pi$  interactions, electron donor-acceptor interactions, electrostatic attraction, hydrogen-bonding, hydrophobic partitioning, and pore-filling effects [7,32,39–41]. Previous studies have shown that rice husk biochar

can effectively reduce water-soluble and exchangeable Cu (25.8%), Zn (44.8%), Cr (67%) and Cd (85%) in heavy metal-contaminated soil [42]. Peanut shell biochar could reduce exchangeable Pb by 42.0%, exchangeable Cd by 35.7% and exchangeable Cu by 31.9% [43]. Also, biochar produced from wheat straw achieved a degradation rate of 73.9 and 75.1% for phenanthrene and benzene in actual soil, respectively [44]. However, the adsorption performance of virgin biochar remains limited [32,45], and further improvements in its adsorption capacity for pollutants is quite necessary. So far, various modification methods to positively alter the structure and properties of biochar for the remediation of pollutant in water and soil have been widely studied [45–48]. However, the summaries on the modification of biochar and its remediation of heavy metals and organic pollutants in soil are still not comprehensive enough, especially for the reaction mechanism. The mechanistic differences between the immobilization of heavy metals and the removal of organic pollutants have not been comparatively discussed in a comprehensive manner. Moreover, field applicability, economic feasibility and the performance of biochar under multi-pollutant conditions still remain insufficiently addressed.

Thus, the progress in the preparation and modification of biochar are summarized in this study, including studies on pore structure, surface functional groups, surface charge and magnetization modification methods. Further, the role of biochar modification in the adsorption mechanism of heavy metals and organic pollutants was also summarized, and field-scale application and economic considerations were also discussed. The conceptual framework of this review is shown in Figure 1. The main aims were to (1) integrate biochar preparation methods with four representative modification strategies and link them to pollutant-specific physicochemical properties; (2) illustrate the mechanistic differences between heavy metal immobilization and organic pollutant removal in soil; (3) extend the discussion from laboratory-scale mechanisms to field application, aging effects, ecological risk, and economic feasibility, thereby providing a more application-oriented framework for biochar-based soil remediation to support safer agricultural production and sustainable soil management.

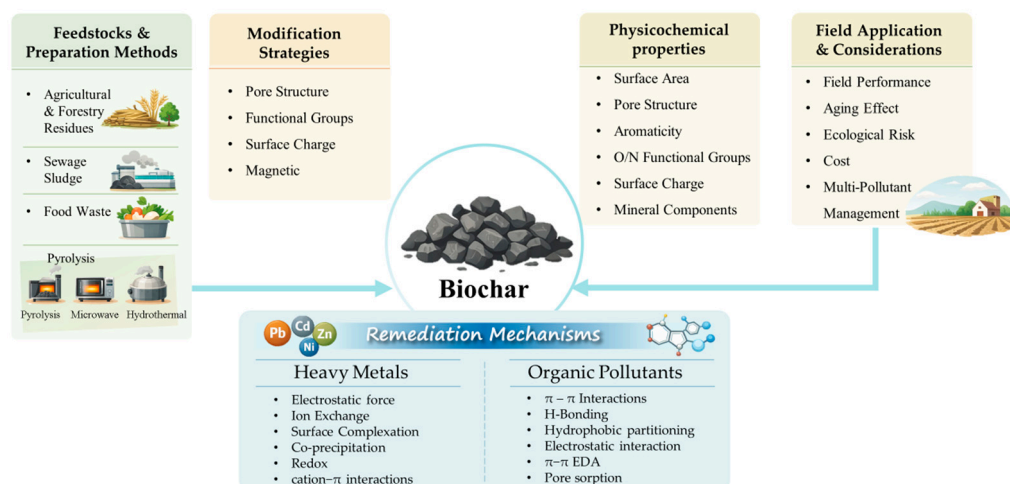


**Figure 1.** Conceptual framework linking feedstocks and preparation methods, modification strategies, physicochemical properties, remediation mechanisms and field-scale application considerations of biochar for soil remediation.

## 2. Materials and Methods

A literature search was conducted using the Web of Science, PubMed, Google Scholar, and ScienceDirect databases. The main search terms included “biochar”, “soil remediation”, “heavy metals”, “organic pollutants”, “biochar modification”, “adsorption mechanism”,

“field application”, and “economic feasibility”. Peer-reviewed research articles and representative review papers published from 2010 to 2025 were mainly encompassed and a few earlier classic and foundational references were also included when necessary. Particular emphasis was placed on recent studies related to the preparation, modification, remediation mechanisms and field-scale applications of biochar in contaminated soils. Relevant references cited in the selected articles were also examined to improve the coverage of the review.

### 3. Biochar Preparation Methods

The raw materials for biochar are primarily from agricultural and forestry waste and food residues like fruit shells and straw. Biochar not only demonstrates its environmentally friendly characteristics but also achieves the resource utilization of waste, thereby reducing the costs associated with pollution remediation [49–51]. The main methods for preparing biochar include thermal pyrolysis, microwave pyrolysis and hydrothermal carbonization [52].

#### 3.1. Conventional Pyrolysis

Pyrolysis is a process that involves decomposing biomass feedstocks such as fruit peels, corn stalks and peanut shells at high temperatures under an inert gas atmosphere. During this process, the chemical bonds within the biomass break down, leading to the release of moisture, organic matter and volatile components, thereby producing biochar. As the pyrolysis temperature increases, the pore structure of biochar becomes more complex, its specific surface area and aromaticity generally increase, and its surface functional groups and elemental composition also undergo significant changes [48,53,54]. Conventional pyrolysis is generally suitable for relatively dry lignocellulosic biomass. Typical feedstocks include crop straw, wood chips, sawdust, nutshells, corn stalks and peanut shells [55–57]. These feedstocks are easy to preprocess and usually produce biochar with a relatively high carbonization degree, aromaticity and structural stability.

#### 3.2. Microwave Pyrolysis

Microwave pyrolysis is an emerging heating technology that employs a non-contact microwave energy transfer method. Biochar is served as a microwave absorber capable of efficiently absorbing microwaves and converting them into thermal energy. Molecular friction and collisions among water molecules in biomass generate a heating effect that drives the pyrolysis reaction under microwave radiation. These biomass materials undergo pyrolysis to form biochar through thermal contact with the microwave absorber [58]. Microwave pyrolysis is more suitable for biomass with favorable dielectric properties, moderate moisture content, or good microwave absorption behavior. Common feedstocks include agricultural and forestry residues, wood biomass, crop residues, bamboo sawdust and other lignocellulosic materials [59–61]. For feedstocks with poor microwave responsiveness, additional microwave absorbers are often needed.

#### 3.3. Hydrothermal Carbonization

Hydrothermal carbonization is a biomass conversion method that uses water as a reaction medium, which undergoes a series of complex thermochemical conversion processes to convert biomass feedstock into hydrothermal carbon, liquid oil and gas under controlled temperature, time and pressure conditions [62]. Different types of biomass feedstock and preparation methods confer distinct physical and chemical properties on biochar, leading to specific adsorption efficiency of various pollutants in the remediation applications. The conversion process mainly involves hydrolysis, dehydration, decarboxylation, condensation/polymerization, and progressive aromatization of biomass under

hydrothermal conditions. These processes are closely associated with the carbonization degree, oxygen-containing functional groups, mineral retention and surface pore distribution of the resulting hydrochar, thereby affecting its remediation performance [62–64]. Hydrothermal carbonization of biochar is a complex process, generally evaluated in terms of process parameters, material structure and properties, and remediation performance, rather than through an in-depth discussion of its thermochemical processes. Accordingly, this review mainly focused on the effects of preparation methods and feedstock types on biochar properties relevant to soil remediation applications. Hydrothermal carbonization is particularly suitable for high-moisture biomass. Typical feedstocks include sewage sludge, manure, food waste, algal biomass, digestate, municipal waste and other wet organic residues [65,66]. This method can directly process wet feedstocks under aqueous conditions and avoids energy-intensive drying pretreatment.

#### 4. Biochar Activation and Modification

In this section, the detailed activation approaches such as steam treatment, CO<sub>2</sub> activation, and chemical etching, as well as modification strategies including surface functionalization, charge regulation, and magnetic loading are discussed.

##### 4.1. Pore Structure Activation and Modification

The activation of biochar pore structure generally involves changes in specific surface area, pore volume, shape and pore size distribution function [33,67,68]. Pore structure activation can be categorized into physical and chemical activation, which utilizes steam activation and CO<sub>2</sub> to treat biochar to increase its pore volume and specific surface area, while avoiding the introduction of chemical substances and preserving the natural properties and environmental friendliness of biochar. Shao et al. analyzed the pore structure of corncob biochar activated with CO<sub>2</sub> and found that, compared to unmodified biochar, the modified biochar exhibited a 13-fold increase in specific surface area and a 19-fold increase in microporous pore number [69]. Similarly, steam activation increased the specific surface area of giant Miscanthus biochar from 181 to 322 m<sup>2</sup>·g<sup>-1</sup>, indicating that gaseous activation can effectively open pore structures [70]. Physical activation methods could effectively improve the pore distribution and structure of biochar while remaining environmentally friendly. Chemical modification methods primarily involve using acid-base solutions to modify biochar and improve its pore structure, increasing the specific surface area of the pores [71]. The most commonly used chemical modifiers mainly include alkaline agents such as KOH and NaOH and acidic reagents such as H<sub>3</sub>PO<sub>4</sub>, HCl, and HNO<sub>3</sub> in previous studies [72,73]. Zhang et al. utilized hydrofluoric acid degassing and potassium acetate modification to improve the pore structure of sludge biochar. Due to the combined effects of hydrofluoric acid washing and the etching of SiO<sub>2</sub> and potassium acetate, the specific surface area of the modified biochar increased 12-fold [74]. Furthermore, KOH modification of corn straw biochar produced a highly porous material with a specific surface area of 2183.80 m<sup>2</sup>·g<sup>-1</sup> and abundant micropores mainly distributed at 1–2 nm [75]. NaOH modification was also found to expand and optimize the pore structure on the biochar surface by increasing the number of active adsorption sites (Figure 2) [76]. Acid-base modifiers alter the surface morphology and improve the pore structure of biochar through etching, resulting in a significant increase in the specific surface area and size of biochar pores, thereby improving its adsorption performance. Although chemical modification can effectively enhance the adsorption performance of biochar, its environmental risks must be assessed in practical applications to avoid secondary environmental pollution.

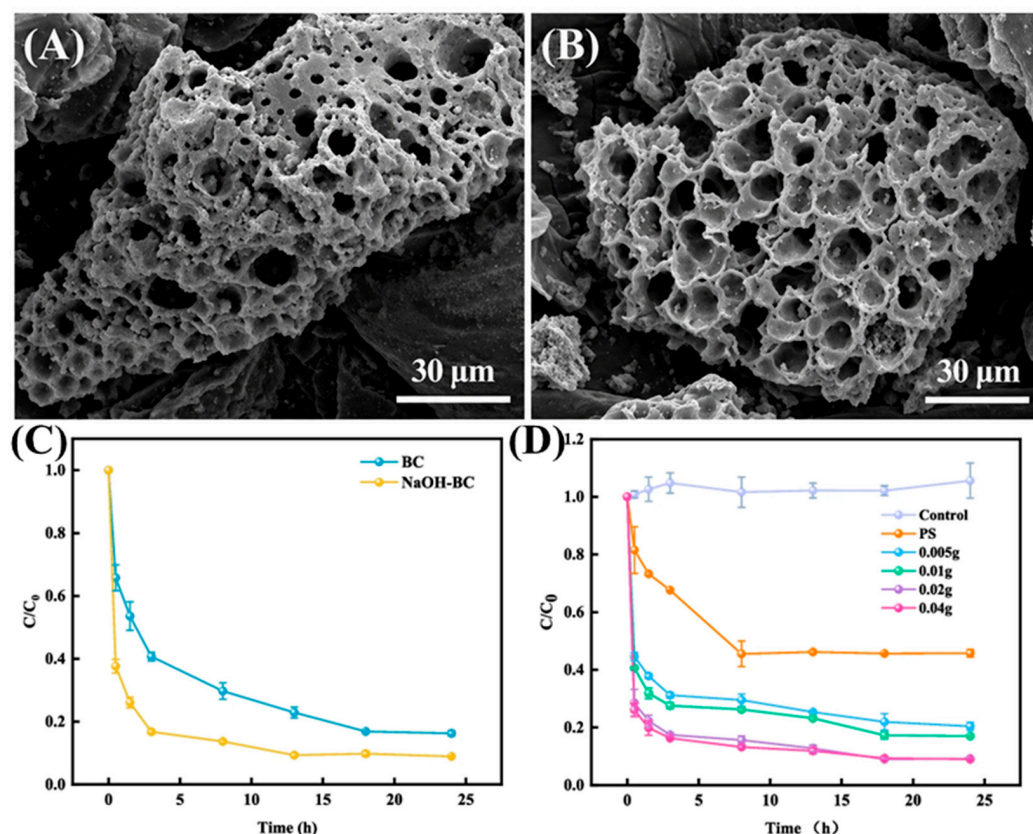


**Figure 2.** SEM images of different samples: (A) unmodified BC, (B) NaOH-modified biochar, (C) comparison of BC and NaOH-BC on DBP degradation in soil, (D) effect of different NaOH-BC additions on DBP degradation in persulfate (PS) solution [76].

#### 4.2. Surface Functional Group Modification

Introducing functional groups onto the surface of biochar can enhance its adsorption performance for soil pollutants. The primary functional groups include oxygen-containing and nitrogen-containing groups, and these modified biochar can effectively form these functional groups on its surface [36]. Sanford et al. found that NaClO can oxidize the phenolic groups on the surface of biochar to introduce abundant carboxyl and carbonyl functional groups into the biochar (Figure 3) [77]. Additionally, nitro ions form stable complexes with the aromatic benzene ring  $\pi$ -electron system of carbon-based groups under the influence of aromatic electrophilic substitution reactions, thereby effectively grafting nitro functional groups [78]. Nitrogen dopants can introduce nitrogen-containing functional groups, and common nitrogen dopants include melamine, ammonium chloride and urea, which introduce pyridine groups to biochar and enhance aromaticity [78–82]. Zhou et al. observed N–H and C–N vibration peaks in polyethyleneimine-modified bamboo charcoal materials via FT-IR. The protonation of amino groups imparts a positive charge to the biochar surface, enabling it to attract negatively charged Cr(VI) ions, and unprotonated amino groups can form hydrogen bonds with Cr(VI) [83]. Surface functional group modification can significantly improve the surface properties of biochar for enhancing its adsorption capacity for pollutants. However, the adsorption enhancement induced by surface functional group modification is contaminant-specific. For example, increasing oxygen-containing functional groups on the biochar surface through modification can enhance the adsorption of polar or ionic organic pollutants [84], whereas this might conversely inhibit the adsorption of aromatic or nonpolar organic pollutants by biochar [85]. Thus, the design of surface functional group modification should be tailored to the physicochemical properties of the target contaminants.

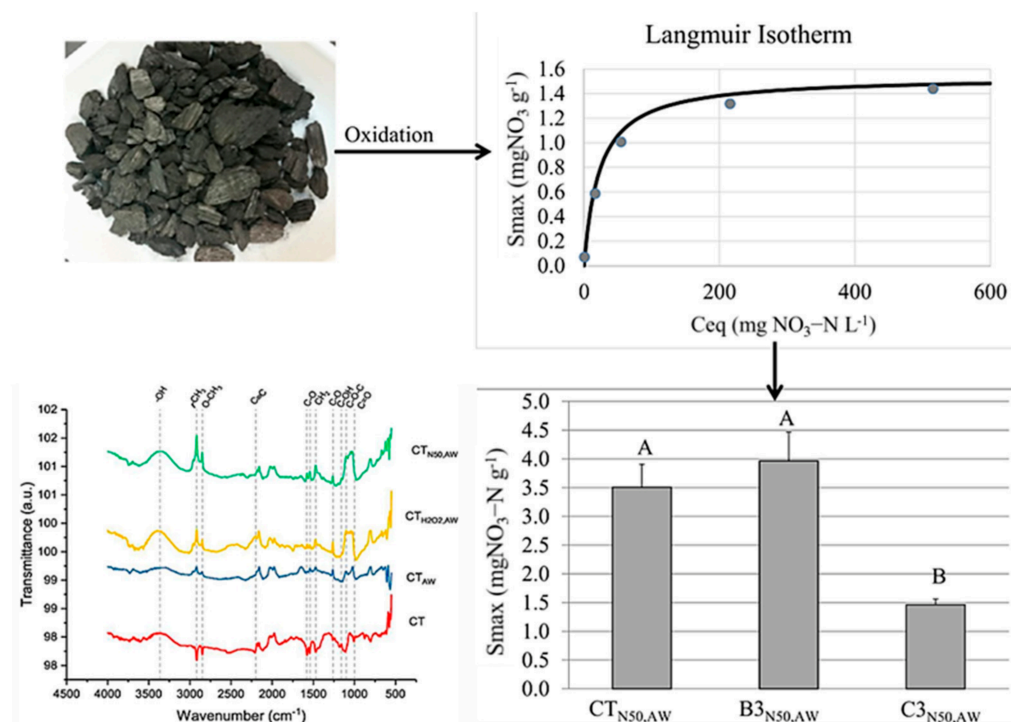


**Figure 3.** FT-IR spectra for CT, CT<sub>AW</sub>, CT<sub>H<sub>2</sub>O<sub>2</sub></sub>, CT<sub>AW</sub>, and CT<sub>N50,AW</sub>. CT: Carbon Terra biochar, AW: Acid wash, H<sub>2</sub>O<sub>2</sub>: Oxidize with 50 mmol·g<sup>-1</sup> H<sub>2</sub>O<sub>2</sub>, N50: Oxidize with 50 mmol·gBC<sup>-1</sup> NaClO, error bars represent standard deviation of replicates. Letters signify significant difference ( $p < 0.05$ ) between Smax values [77].

#### 4.3. Surface Charge Modification

Changes in the surface charge properties of biochar are typically associated with environmental pH, which are also closely related to its point of zero charge (pHpzc) and zeta potential; these parameters jointly determine the electrostatic attraction or repulsion of biochar toward ionic pollutants. It has been reported that addition of biochar to soil can increase soil pH by 0.3–1.7 units in heavy metal soil (Figure 4) [86]. Biochar modified with weak acid salts can significantly increase soil pH, promoting the formation of heavy metal precipitates and inhibiting adsorption competition among multiple heavy metals when they coexist [87]. Additionally, surface charge can be altered through coating modification. Wu et al. found that as the coating of fulvic acid (FA) increased, the number of positive charge groups on the biochar surface decreased, and the Zeta potential curves of FA-PBs as a function of pH were similar to that of free FA [88]. Surface charge regulation is also important for ionic organic pollutants. PFOS adsorption by red mud-modified sawdust biochar was enhanced under acidic conditions below pHpzc because protonated surface groups and positively charged metal-oxide sites promoted electrostatic attraction [89]. Biochar can effectively achieve efficient adsorption of target pollutants in pH by regulating surface charge. However, surface charge effects are easily influenced by ionic strength, coexisting ions and dissolved organic matter, and are generally less stable than complexation, precipitation or redox mechanisms. In addition, modification of the surface charge of biochar mainly affects its electrostatic attraction toward ionic pollutants, whereas donor-acceptor interactions and cation- $\pi$  interactions arise from electron-rich aromatic structures and surface functional groups; these mechanisms are discussed separately in the mechanistic section.

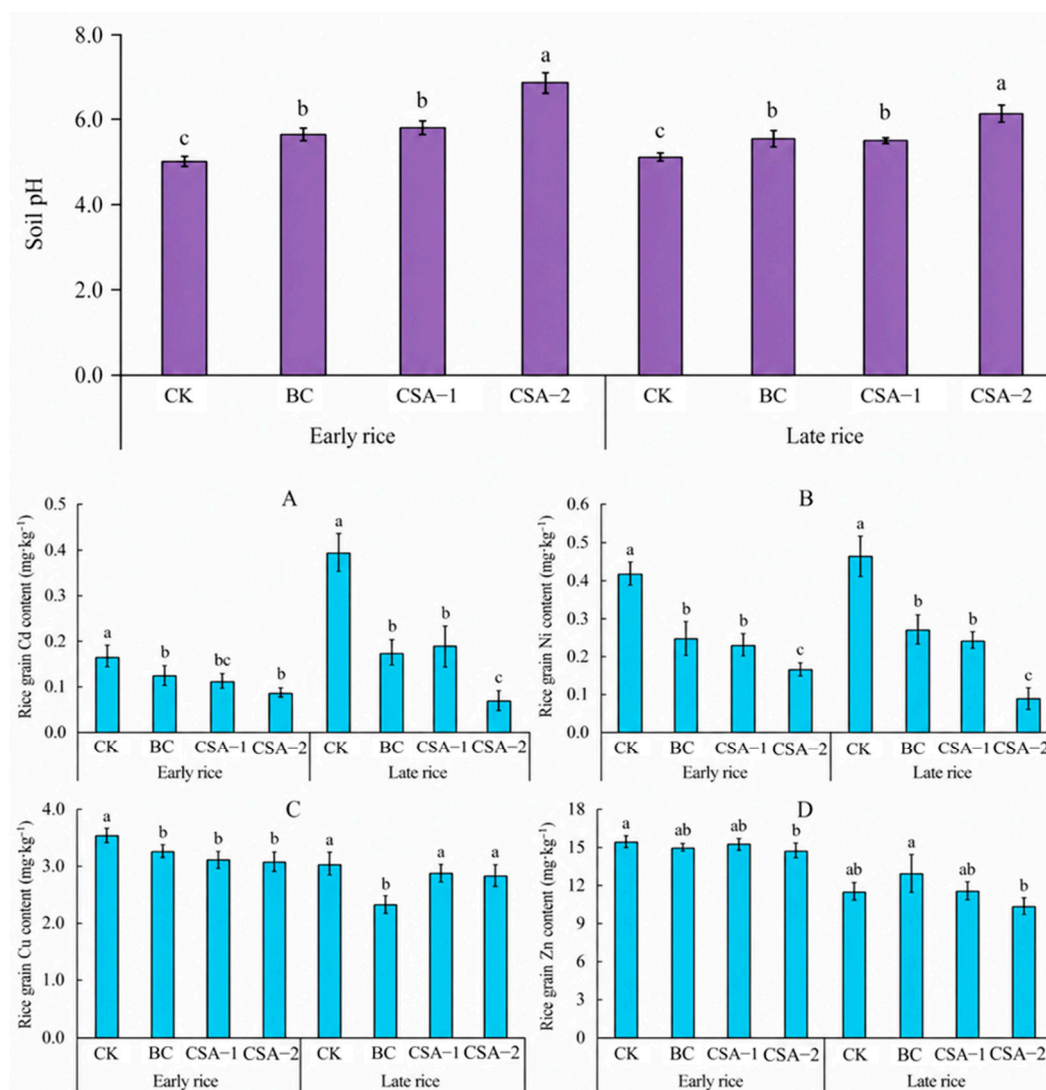


**Figure 4.** Effects of soil pH changes on Cd (A), Ni (B), Cu (C) and Zn (D) content in early rice and late rice grain. CS-1: 0.5%, a composite material consisting of biochar, limestone, sepiolite, and potassium dihydrogen phosphate, CSA-2: 1%, a composite material consisting of biochar, limestone, sepiolite, and potassium dihydrogen phosphate, Different letters indicate significant differences ( $p < 0.05$ ) between treatments in each growth season [86].

#### 4.4. Magnetic Modification

Magnetic modification of biochar involves attaching or embedding magnetic materials onto biochar materials, which not only enhances the biochar's ability to adsorb pollutants but also provides it with recyclable and reusable functionality. The magnetic properties of modified biochar are commonly evaluated by parameters such as saturation magnetization, remanence and coercivity, which directly reflect its magnetic responsiveness, separability and potential reusability [90]. Liang et al., using magnetic biochar to remediate As-contaminated paddy soil, found that the material exhibited a magnetization close to 1.75 emu, indicating that the magnetic biochar possessed recoverable properties. Moreover, the remanence and coercivity were both zero, suggesting that the material was not prone to irreversible aggregation caused by residual magnetism and exhibited superparamagnetic characteristics favorable for repeated recovery and reuse [91]. In addition, XRD, XPS, SEM-EDS and magnetic hysteresis measurements are often used to confirm the formation, distribution and magnetic behavior of Fe-based phases on the biochar surface [92]. The main methods for imparting magnetic properties to biochar include impregnation pyro-

sis, hydrothermal synthesis, co-precipitation and liquid-phase reduction [93]. Tang et al. loaded Fe<sub>3</sub>O<sub>4</sub> onto mulberry stem biochar by precipitating Fe<sup>2+</sup>/Fe<sup>3+</sup> with ammonia solution, and the resulting Fe<sub>3</sub>O<sub>4</sub>@MBC could effectively immobilize As in highly contaminated paddy soil (Figure 5) [94]. Diao et al. loaded nano-zero-valent iron (nZVI) onto biochar to produce iron-modified biochar. It was found that iron-modified biochar not only significantly reduced the agglomeration effect of nano-zero-valent iron, but also enhanced the adsorption performance of Cr(VI) and Pb(II) with a removal rate of over 70% even after three reuses [95]. Magnetically modified biochar combines the advantages of efficient removal and recyclability, demonstrating excellent application potential in environmental pollution control.

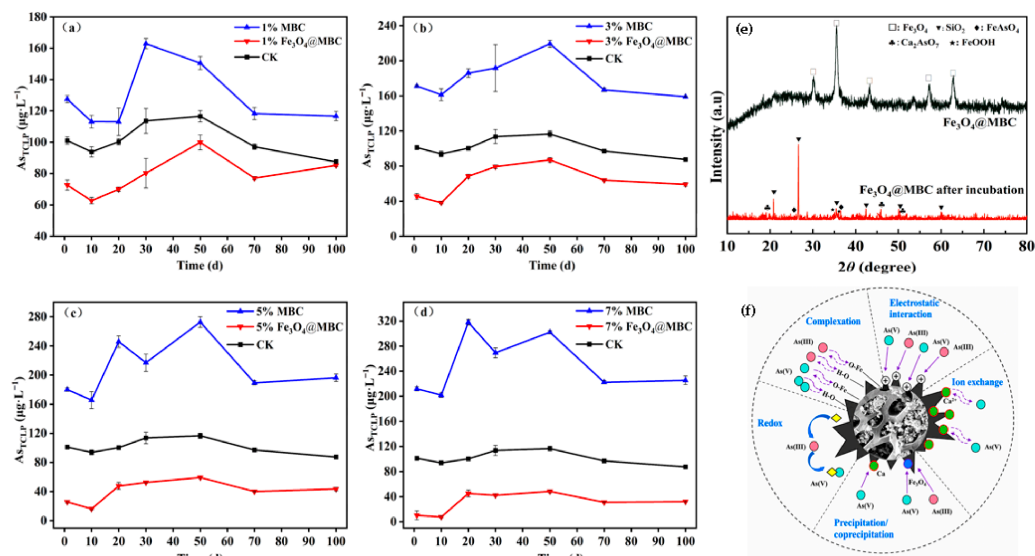


**Figure 5.** (a–d)  $As_{TCLP}$  content change of 1%, 3%, 5%, 7% MBC and Fe<sub>3</sub>O<sub>4</sub>@MBC-amended soil in 1–100 d, (e) XRD spectra of pristine Fe<sub>3</sub>O<sub>4</sub>@MBC and Fe<sub>3</sub>O<sub>4</sub>@MBC after 100 d of incubation, (f) the proposed mechanism of Fe<sub>3</sub>O<sub>4</sub>@MBC remediation for arsenic-contaminated soil, MBC: mulberry stem powder biochar, Fe<sub>3</sub>O<sub>4</sub>@MBC: magnetic modification biochar [94].

A summary of representative activation and modification strategies, key characterization evidence, and corresponding biomass feedstocks for soil remediation is provided in Table 1.

**Table 1.** Representative biochar activation and modification strategies, major characterization evidence, and corresponding biomass feedstocks for soil remediation.

Biochar	Modification Type	Modification Method	Key Characterization	Reference
Corn cob	Pore structure	CO <sub>2</sub> activation and amine impregnation	BET showed the specific surface area increased from 56.91 to 755.35 m <sup>2</sup> g <sup>-1</sup> .	[69]
Sewage sludge	Pore structure	HCl/HF deashing and potassium acetate activation	BET showed the specific surface area increased from 81.35 to 223.65 m <sup>2</sup> g <sup>-1</sup> .	[74]
Wood/corn cob	Surface functional group	NaClO/H <sub>2</sub> O <sub>2</sub> oxidation	The FT-IR spectra shows a clear increase in oxygenated functional groups for modified biochar.	[77]

Table 1. Cont.

Biochar	Modification Type	Modification Method	Key Characterization	Reference
Waste rice straw	Surface functional group	Nano-hydroxyapatite loading	The FT-IR spectra shows a clear increase in oxygenated functional groups for modified biochar.	[83]
Platane wood	Surface charge	Fulvic acid coating	The zeta potentials indicated that modification decreased the number of positively charged groups on the biochar surface.	[88]
Sawdust	Surface charge	Red mud/ metal-oxide coating	The kinetic fitting results indicated that electrostatic interactions dominated adsorption.	[89]
Sewage sludge	Magnetic	nZVI immobilization	The XRD patterns revealed the formation of Fe <sup>0</sup> particles on the biochar surface.	[95]
Crayfish shell	Magnetic	Fe composite via ferric chloride	SEM-EDS spectra indicated that Fe was successfully loaded onto the biochar via modification.	[52]

## 5. Mechanism Remediation of Heavy Metals and Organic Pollutants in Soil by Biochar

### 5.1. Adsorption of Heavy Metals

Extensive human production activities have led to the introduction of large amounts of heavy metals into soil, which poses risks to human health and ecological safety. Many studies indicated that biochar has been widely applied for the remediation of heavy metals such as Cr(VI), Cd(II), Cu(II), Pb(II) and As(III) in contaminated soil, which well demonstrates its highly efficient remediation performance. Zhou et al. utilized a composite material made from hydroxyapatite and biochar for the adsorption of Cr(VI) and Pb(II) in soil. The adsorption efficiency for Pb(II) reached 89% with the primary adsorption mechanisms being complexation and cation- $\pi$  interactions [83]. Diao et al. studied the removal of Cr(VI) and Pb(II) using sludge biochar immobilized with nano-zero-valent iron, and found that the primary removal mechanism was reduction and surface precipitation [95]. The adsorption performance of different modified biochar on heavy metals is shown in Table 2. The removal mechanism of biochar for heavy metals in soil primarily includes electrostatic interactions, cation- $\pi$  interactions, complexation, ion exchange and surface precipitation (Figure 6) [88–97].

Table 2. Remediation of heavy metals in soil by biochar.

Biochar	Pollutants	Mechanism	Performance	Reference
Straw	Cd, Pb	Electrostatic adsorption	The maximum adsorption capacity of 65.2 mg·g <sup>-1</sup> for Cd and 178.7 mg·g <sup>-1</sup> for Pb, respectively.	[98]
Red mud and maple wood	Cu, Pb	Electrostatic adsorption	The maximum adsorption capacity of 80 mg·g <sup>-1</sup> for Cu and 92.59 mg·g <sup>-1</sup> for Pb, respectively.	[99]
Corn straw	Cd, Zn	Surface complexation	Bioavailable Cd and Zn were reduced by 57.79% and 35.64%, respectively.	[100]

Table 2. Cont.

Biochar	Pollutants	Mechanism	Performance	Reference
<i>Spartina alterniflora</i>	Cd	Surface complexation	Bioavailable Cd was decreased by 24%.	[101]
Corn stalk	Cd	Cation- $\pi$ interaction	The maximum adsorption capacity of 23.54 mg·g <sup>-1</sup> for bioavailable Cd.	[102]
Rice straw	Pb	Surface complexation	The maximum adsorption capacity of 35.03 mg·g <sup>-1</sup> for bioavailable Pb.	[83]
Cotton stalk	Cd	Ion exchange	The maximum adsorption capacity of 664.6 mg·g <sup>-1</sup> for Cd.	[103]
Fish scales	Cd	Ion exchange	Bioavailable Cd was decreased by 60%.	[104]
<i>Myriophyllum verticillatum</i> L.	Pb	Co-precipitation	The maximum adsorption capacity of 45.61 mg·g <sup>-1</sup> for Pb.	[105]
Kenaf bar	Cd, Pb	Surface complexation	Bioavailable Cd and Pb were reduced by 49% and 45%.	[33]
Corn straw	Cr	Redox transformation	The adsorption capacity for Cr(VI) in soil reached 335.55 mg/g.	[106]
Bamboo powder	As	Redox transformation	Bioavailable As was reduced by 54.56%.	[107]

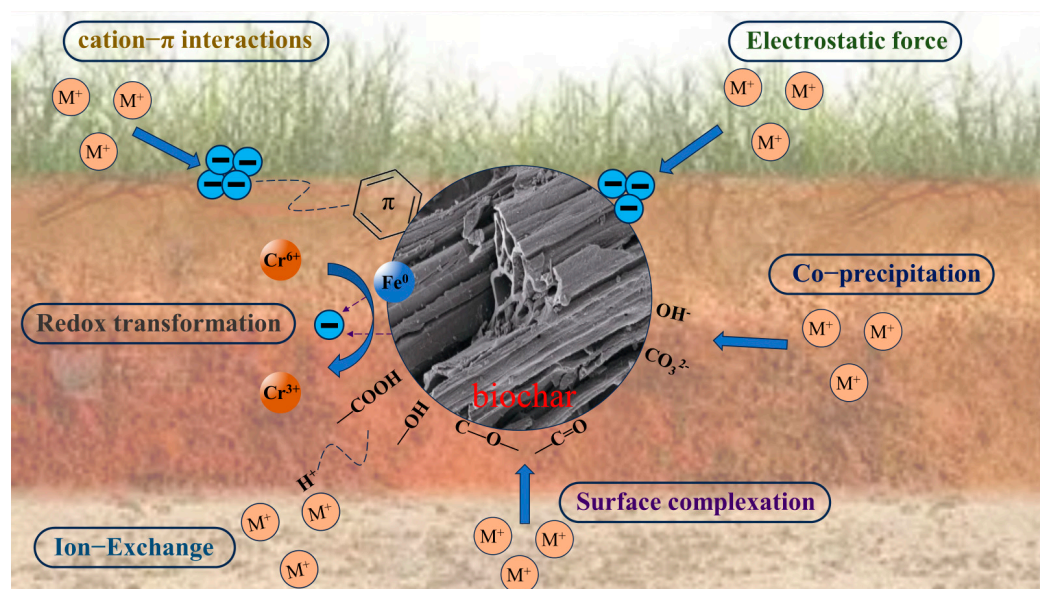


Figure 6. Mechanism of heavy metal adsorption by biochar in soil.

#### 5.1.1.1. Electrostatic Interaction

Biochar with negatively charged surfaces tends to undergo electrostatic adsorption with positively charged heavy metal ions such as  $\text{Hg}^{2+}$ ,  $\text{Pb}^{2+}$  and  $\text{Cd}^{2+}$ . Conversely, biochar with positively charged surfaces tends to undergo electrostatic adsorption with negatively charged heavy metal ions like  $\text{Cr}_2\text{O}_7^{2-}$ . Electrostatic interactions are also influenced by soil pH. When soil pH is low, biochar becomes positively charged due to the protonation of surface functional groups for the enhancement of electrostatic adsorption of heavy metal acid anions such as  $\text{HAsO}_4^{4-}$ ,  $\text{Cr}_2\text{O}_7^{2-}$  and  $\text{Sb}(\text{OH})_6^-$  [108,109]. Anum et al. found that nitrogen-doped modification could lower the zero-charge pH of biochar, enabling it to carry a negative charge over a broader range of pH [98]. Nitrogen and oxygen-containing groups can modify the surface charge distribution of biochar and provide additional binding sites, thereby enhancing its electrostatic attraction and surface complexation toward

available Cd and Pb in soil. Chakma et al. found that acid modification can introduce acidic oxygen-containing functional groups to the biochar surface for enhancing electrostatic interactions with metal ions. However, compared to strong interactions such as complexation, electrostatic interactions might not be the primary mechanism for the adsorption of heavy metals by biochar [99]. The competitive interactions between pollutants are also prominent in soil environments where multiple pollutants coexist [105]. Therefore, the weak bonding characteristics of the electrostatic interaction mechanism and its limitations in competitive adsorption when multiple pollutants coexist restrict its role as the primary removal mechanism and its stable efficacy in actual pollutant remediation.

#### 5.1.2. Complexation

The complexation of heavy metals involves the interaction between heavy metal ions and various ligands, which directly influences the migration, transformation and bioavailability of heavy metals in soil. The hydroxyl-, carboxyl- or nitrogen-containing functional groups on biochar surface can provide abundant binding sites for heavy metal ions, leading the formation of complexes with metal ions to achieve heavy metal remediation. Kang et al. found that CdO diffraction peaks appeared on the iron–manganese-modified biochar after the reaction using XRD; the result indicated that complexation exists during this biochar adsorption process, and iron–manganese modification introduced abundant oxygen-containing functional groups to the biochar surface making complexation the primary remediation mechanism [100]. Qiu et al. found that both –OH and –COOH groups on the biochar surface can be formed by complexation with Cd<sup>2+</sup> via coordinate bonds, and the Al and Si in kaolinite can also complex with Cd<sup>2+</sup> in the soil to form complexes [101]. Chelation is also widely present in the adsorption of heavy metals by minerals like goethite and kaolinite, and mineral loading and doping can be utilized to enhance the chelation of heavy metals by biochar.

#### 5.1.3. Cation– $\pi$ Interaction

During the pyrolysis process, biochar can form a large number of aromatic ring structures, which are rich in  $\pi$  electrons, and can interact with heavy metal ions such as Pb<sup>2+</sup>, Cd<sup>2+</sup> and Cu<sup>2+</sup> through electrostatic attraction and charge transfer. Zhou et al. found that nano-hydroxyapatite-modified biochar adsorb Pb<sup>2+</sup> and Cd<sup>2+</sup> from soil, and the interaction between these heavy metal ions and the  $\pi$  bonds of biochar weakened the electron density around the C=C bonds, causing the adsorbed C=C spectral bands to shift to higher binding energies, which indicated the presence of cation– $\pi$  interactions [83]. Chemically modified amine-modified biochar can also indirectly enhance the cation– $\pi$  interaction between aromatic biochar and Cd<sup>2+</sup> by increasing contact with Cd<sup>2+</sup> [102]. Cation– $\pi$  interactions play a significant role in the adsorption of heavy metals over biochar, and the optimization of conditions for this mechanism should be considered during the high-temperature pyrolysis process of biochar preparation.

#### 5.1.4. Ion Exchange

Ion exchange typically occurs between H<sup>+</sup> ions and heavy metal ions at functional groups on the surface of biochar, such as hydroxyl and carboxyl groups. These functional groups provide H<sup>+</sup> ions to react with heavy metal ions to form stable metal complexes, thereby reducing the mobility of heavy metals in soil. Su et al. found that the ion exchange capacity of manganese-modified bamboo biochar could be enhanced due to the oxidation of its surface functional groups [103]. Gao et al. compared the adsorption mechanisms of Pb<sup>2+</sup> by cotton stalk biochar before and after acid washing, and the results showed that the inorganic components on the unwashed biochar undergo ion exchange with Pb<sup>2+</sup> to form lead carbonate and hydroxyphosphate lead, while the surface of acid-washed

biochar did not exhibit significant ion exchange activity [110]. Additionally, ion exchange also occurs between the mineral components on the surface of biochar and heavy metal ions. The mineral components on the surface of biochar like hydroxyapatite facilitate the adsorption of heavy metal ions from soil. Xiao et al. used fish scale biochar self-doped with hydroxyapatite and loaded with MgO to adsorb  $\text{Cu}^{2+}$ ,  $\text{Cd}^{2+}$  and  $\text{Pb}^{2+}$  from soil. It was found that  $\text{Ca}^{2+}$  and  $\text{Mg}^{2+}$  on the biochar could adsorb  $\text{Cu}^{2+}$ ,  $\text{Cd}^{2+}$  and  $\text{Pb}^{2+}$  from soil through ion exchange and then precipitate these heavy metal ions [104]. Addition of high-valent metal ions or doping with soluble minerals can enhance the ion exchange capacity of biochar during the adsorption of heavy metal ions by biochar.

#### 5.1.5. Surface Precipitation

The specific ions present on the surface of biochar bind with heavy metal ions to form insoluble precipitates [95]. Zhang et al. found that biochar can promote the formation of  $\text{Cd}^{2+}$  carbonates or hydroxides by increasing soil pH and providing mineral components such as  $\text{Ca}^{2+}$  and  $\text{Mg}^{2+}$  [111]. Metal salt modification agents such as potassium permanganate can enrich biochar with metal cations such as  $\text{K}^+$ ,  $\text{Na}^+$ ,  $\text{Ca}^{2+}$ ,  $\text{Mg}^{2+}$  and  $\text{Mn}^{2+}$ , enhancing biochar's ability to precipitate heavy metals such as Cd and Pb in soil [112]. Qian et al. found that the loading of nano-zero-valent iron provided biochar with abundant oxygen-containing functional groups, which can increase soil pH and promote the formation of hydroxide and carbonate precipitates of  $\text{Cd}^{2+}$  and  $\text{Pb}^{2+}$  [33]. Biochar can enhance the surface precipitation of heavy metal ions in soil through modification. The surface precipitation mechanism exhibits good resistance to aging and often serves as the primary adsorption mechanism under high-pollution conditions [113]. Modification strategies such as metal salt modification or nano-zero-valent iron loading significantly enhance the surface precipitation of heavy metals like  $\text{Cd}^{2+}$ ,  $\text{Pb}^{2+}$  and  $\text{Cu}^{2+}$  by strengthening biochar's pH regulation capacity and providing precipitation ion components. Given its excellent anti-aging performance and dominant role in highly polluted scenarios, precipitation is an indispensable key pathway for biochar-based heavy metal stabilization.

#### 5.1.6. Redox Transformation

Redox transformation is not a simple adsorption process. Instead, biochar acts as an electron donor, electron shuttle, or redox catalytic medium to transform highly toxic and bioavailable metal(loid)s into less toxic and less mobile species, which are subsequently immobilized through surface complexation and/or precipitation. Biochar-based materials can reduce highly toxic Cr(VI) to the less toxic Cr(III), which is then fixed by surface functional groups or retained as precipitated phases [106]. Nanoscale zero-valent iron-modified corn stalk biochar exhibited a maximum Cr(VI) uptake of  $352.44 \text{ mg}\cdot\text{g}^{-1}$  in soil remediation systems [114]. As(III) in soil can also be oxidized and subsequently immobilized by biochar-based materials. Fe-modified biochar showed that the proportion of As(III) in soil decreased to 54.56% under oxidative treatment, where surface quinone and carbonyl groups promoted the oxidation of As(III) to As(V), followed by the formation of  $\text{FeAsO}_4$  and  $\text{Fe}_3\text{AsO}_7$  [107]. The removal of Sb(III) in soil can proceed through a similar redox-assisted pathway [115,116]. It should be noted, however, that oxidized or reduced metal(loid)s may still retain potential mobility. Redox transformation usually operates synergistically with surface complexation on Fe/Mn oxides, co-precipitation and an increase in residual fractions.

### 5.2. Adsorption of Organic Pollutants

Large amounts of organic pollutants such as pesticides, phenols, dyes, endocrine disruptors, polycyclic aromatic hydrocarbons and antibiotics remain in the soil. These organic pollutants can disrupt biological metabolism, damage biological systems, and

even pose a carcinogenic risk. Biochar has also been widely applied in the remediation of organic pollutants in soil, and has well demonstrated a highly effective remediation performance. Yao et al. found that sugarcane bagasse biochar using hydrothermal carbonization and  $ZnCl_2$  activation method exhibited a high adsorption capacity for toluene with  $435.812 \text{ mg}\cdot\text{g}^{-1}$  with primary adsorption mechanism being pore filling [71]. Liu et al. studied the removal of methylene blue using manganese-modified lignin biochar and found that the adsorption capacity of methylene blue was  $248.96 \text{ mg}\cdot\text{g}^{-1}$  with the primary adsorption mechanism being electrostatic adsorption and hydrogen-bonding effects [117]. The organic pollutants' adsorption performance of biochar from soil is shown in Table 3. The adsorption mechanism of biochar primarily includes  $\pi$ - $\pi$  interactions,  $\pi$ -electron donor-acceptor (EDA) interactions, electrostatic interactions, hydrogen-bonding effects and nanopore-filling effects (Figure 7) [118].

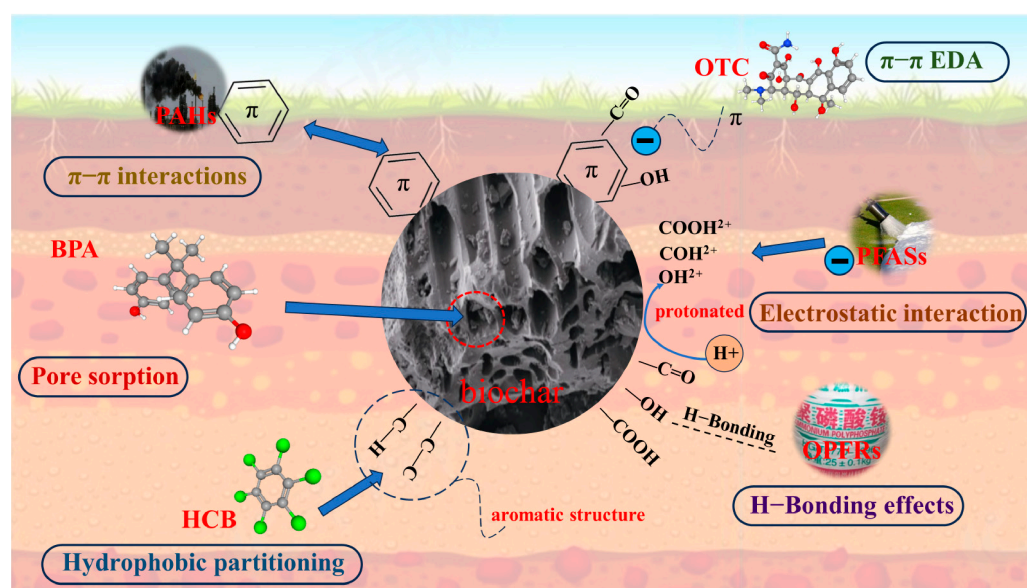


Figure 7. Mechanism of organic pollutant adsorption by biochar in soil.

Table 3. Remediation of organic pollutants in soil by biochar.

Biochar	Pollutants	Mechanism	Performance	Reference
Rice straw	Oxytetracycline	$\pi$ - $\pi$ EDA	The adsorption capacity of biochar for oxytetracycline was $12 \text{ mg}\cdot\text{g}^{-1}$ .	[119]
Rice husk	Polycyclic aromatic hydrocarbons	$\pi$ - $\pi$ EDA	The adsorption capacity of biochar for polycyclic aromatic hydrocarbons was $613 \text{ }\mu\text{g}\cdot\text{kg}^{-1}$ .	[120]
Sorghum stalks	Sulfadiazine	$\pi$ - $\pi$ EDA	The adsorption rate of the biochar for sulfadiazine was 94.4%.	[121]
Wood powder	Cefotaxime	Electrostatic interaction	The adsorption rate of the biochar for cefotaxime was 99%.	[118]
Rice husk	Perfluorooctane sulfonate	Electrostatic interaction	The adsorption capacity of biochar for perfluorooctane sulfonate was $194.6 \text{ mg}\cdot\text{g}^{-1}$ .	[89]
Straw powder	Polycyclic aromatic hydrocarbons	H-Bonding interaction	The adsorption rate of polycyclic aromatic hydrocarbons was 99.3%.	[122]
Bamboo chips	Nitrobenzene, phenols, and anilines	H-Bonding interaction	The adsorption capacity of biochar for sum of the nitrobenzene, phenols, and anilines was $1100 \text{ mg}\cdot\text{g}^{-1}$ .	[123]

Table 3. Cont.

Biochar	Pollutants	Mechanism	Performance	Reference
Waste timber	Per- and polyfluoroalkyl substances	Pore adsorption	Leachate PFAS concentrations were reduced by 98–100%.	[124]
Bamboo biochar	Pentachlorophenol	Hydrophobic partitioning	The methanol- and water-extractable pentachlorophenol concentrations in the soil column decreased by 56% and 65%, respectively.	[125]

### 5.2.1. $\pi$ – $\pi$ Interactions and $\pi$ – $\pi$ EDA Interactions

$\pi$ – $\pi$  interactions occur when the aromatic structures or  $\pi$ -electron clouds on the surface of biochar overlap with the  $\pi$ -electron clouds of organic molecules containing aromatic structures like aromatic hydrocarbons and polycyclic aromatic hydrocarbons, which forms stable intermolecular forces that result in adsorption. Qu et al. used Fe solution magnetic modification of corn stover biochar to adsorb atrazine (ATZ) from soil. It was found that magnetic modification improved biochar structure and enhanced the  $\pi$ – $\pi$  stacking interaction with ATZ containing benzene rings [126].  $\pi$ – $\pi$  EDA interactions are non-covalent interactions formed between electron donors and electron acceptors through the overlap of  $\pi$ -electron clouds. Qin et al. compared the adsorption of oxytetracycline (OTC) by  $\text{H}_3\text{PO}_4$ -modified millet straw biochar produced under different temperature conditions. It was found that high-temperature conditions and  $\text{H}_3\text{PO}_4$  modification could enhance the aromaticity of biochar, thereby improving OTC removal [119]. Additionally, Mazarji et al. used metal–organic frameworks (MIL–101) to modify biochar for the adsorption of polycyclic aromatic hydrocarbons (PAHs) in soil and reached a similar conclusion [120]. Furthermore, the adsorption of biochar for some highly hydrophobic organic pesticides also could be enhanced with the enrichment of its aromatic structure [127]. Compared to  $\pi$ – $\pi$  EDA interactions,  $\pi$ – $\pi$  interactions exhibit weaker strength and easier desorption, which is advantageous for biochar regeneration.

### 5.2.2. Electrostatic Interactions

Electrostatic attraction occurs when the surfaces of biochar and organic pollutants have different charges. In biochar prepared at high temperatures, the primary alkaline functional groups are carbonates and  $-\text{COO}^-$ , while the primary functional groups are  $-\text{O}-$  in biochar prepared at low temperatures; these functional groups confer electronegativity to biochar [128]. Additionally, changes in pH can also influence the electrostatic adsorption of biochar components. It was found that during the adsorption of perfluorooctane sulfonic acid (PFOS) by biochar produced from red mud and sawdust, when pH was below the biochar's zero charge point (pHpzc) and acidic values, the functional groups on the biochar surface are protonated and thus carry a positive charge. Metal-oxide functional groups were formed on the biochar surface due to the red mud modification, which could carry positive charges under acidic conditions, significantly enhancing the adsorption of negatively charged PFOS [89]. Modified biochar can use electrostatic adsorption to remove organic pollutants within a wide pH range, showing promising application prospects.

### 5.2.3. Hydrogen-Bonding Effects

Biochar contains a rich array of functional groups such as hydroxyl, carboxyl and carbonyl groups; these functional groups can form hydrogen-bonding effects with organic compounds containing fluorine, nitrogen, oxygen and other atoms with relatively high electronegativity [84,129]. Du et al. found that the oxygen-containing functional groups

in biochar can act as hydrogen bond receptor sites, forming hydrogen bonds by bridging water molecules with oxygen atoms in organic compounds [130]. Although hydrogen bond energy is an important basis for evaluating the contribution of hydrogen-bonding to the adsorption process, the bonding energy of interaction might vary with factors such as dissolved organic matter (DOM) and changes in soil pH [131]. The role of hydrogen bonding in adsorption behavior is inferred rather than independently calculated in most studies, such as being identified qualitatively by FT-IR and supported semi-quantitatively by XPS-derived oxygen-containing functional group distributions [36,132]. Ke et al. used FT-IR spectroscopy to analyze the adsorption of polycyclic aromatic hydrocarbons (PAHs) by straw biochar loaded with humic acid, and found that hydroxyl groups on the biochar surface act as hydrogen bond donors in the adsorption of PAHs [122]. Hu et al. found that the hydrophilic adsorption sites on the surface of KOH-modified biochar was almost entirely occupied by oxygen-containing functional groups, which could adsorb polar molecules such as amines and phenolic organic pollutants in soil through strong hydrogen-bonding interactions, thereby reducing competition from fulvic acid [123]. Biochar can enhance the contribution of hydrogen-bonding interactions in the adsorption of organic pollutants by increasing surface functional groups and reducing competitive inhibition through modification.

#### 5.2.4. Pore Filling

The pore-filling adsorption of organic pollutants by biochar is primarily governed by the size-matching relationship between pore size and adsorbate molecules, as well as by the specific surface area of biochar. For small organic molecules, such as nitrobenzene, phenol, aniline and 4-nitrophenol, their adsorption was mainly dominated by micropores on the biochar surface [123,133]. In contrast, for larger organic molecules, such as fulvic acid, humic-like dissolved organic matter (DOM) and high-molecular-weight antibiotics, pore filling mainly occurred in mesopores [134–136]. In addition, the specific surface area of biochar determined the adsorption rate and maximum adsorption capacity associated with pore filling [137]. Zhang et al. found that an increase in specific surface area and a decrease in pore size were the primary mechanisms for the adsorption of neonicotinoid pesticides by biochar, which was primarily attributed to a shift from polarity-selective adsorption to porosity-selective adsorption [138]. Sørmo et al. studied the adsorption of per- and polyfluoroalkyl substances (PFAS) from soil by biochar modified using steam activation and CO<sub>2</sub> activation methods. It was found that the biochar's specific surface area was enhanced through two pathways: expanding existing pores and generating new micropores, thereby improving its adsorption capacity for PFAS [124]. Hu et al. studied KOH-modified biochar in competitive adsorption of fulvic acid (FA) and organic pollutants in soil and found that FA was primarily adsorbed via mesopores, with only a 34.6% blockage rate of micropores on the biochar, while nitrobenzene was primarily adsorbed via micropores [123]. Adding biochar to soil can prevent fulvic acid loss while achieving adsorption of organic pollutants.

#### 5.2.5. Hydrophobic Partitioning

When nonpolar or weakly polar organic pollutants encounter biochar with hydrophobic surfaces in soil, they are adsorbed from the aqueous phase of the soil onto the hydrophobic surface of biochar; this process is referred to as hydrophobic partitioning [125]. The extent of hydrophobic partitioning is mainly related to the aromaticity of biochar, as a higher degree of aromaticity provides a more nonpolar surface and a more condensed carbon structure, both of which are more favorable for the retention of hydrophobic organic pollutants [139]. Biochar was found to markedly reduce the volatilization, degradation loss, and earthworm uptake of hexachlorobenzene (HCB) [140]. These findings indicate that, for

strongly hydrophobic organic pollutants such as chlorobenzenes and polycyclic aromatic hydrocarbons (PAHs), hydrophobic partitioning was the dominant mechanism governing their adsorption by biochar in soil [141,142]. Notably, recent studies have increasingly suggested that hydrophobic partitioning often occurs synergistically with mechanisms such as  $\pi$ - $\pi$  interactions and pore filling [143,144], while the introduction of hydrophilic functional groups during biochar aging can substantially weaken the contribution of hydrophobic partitioning to the overall adsorption process [145]. Hydrophobic partitioning is an important mechanism by which biochar reduces the mobility and bioavailability of hydrophobic organic pollutants and pesticides in soil.

## 6. Adsorption/Remediation in Model Multi-Component Systems

In practical soil pollution remediation scenarios, multiple heavy metals or/and organic pollutants often coexist, and the use of biochar in multi-component systems is also summarized.

### 6.1. Multi-Metal Coexisting Systems

In multi-metal systems, different heavy metal ions may compete for sorption sites on biochar, thereby ultimately suppressing the immobilization of individual metals by biochar. For example, the sorption sites of Cd(II) and Ni(II) on biochar largely overlapped, and competition occurred when both metals coexisted in the same system, resulting in a weakened contribution of cation exchange, preferential adsorption of Ni(II) and inhibited adsorption of Cd(II) by biochar [146]. Competition occurs not only among metals, but also between biochar and the soil environment for heavy metals. Meng et al. reported in a ternary soil system containing Cd(II), Cu(II), and Ni(II) that the soil itself also immobilized metals, with the order of  $\text{Cu} > \text{Ni} > \text{Cd}$ , which competed with biochar, whose adsorption order was  $\text{Cd} > \text{Ni} > \text{Cu}$ . They further found that the coexistence of Cu and Ni could further weaken the adsorption and immobilization of Cd(II) by biochar [147]. In addition, the influence of biochar aging on adsorption performance cannot be neglected in practical soil remediation studies. Meng et al. found that the contribution of mineral-associated mechanisms such as ion exchange and surface precipitation gradually decreased with biochar ageing, whereas the adsorption capacity of acidic soil for Cd(II) increased markedly after 0.5 years [37]. Thus, greater attention should be paid to the occupation of sorption sites on biochar in multi-metal systems.

### 6.2. Multi-Organic Coexisting Systems

In multi-organic coexisting systems, organic pollutants in soil often coexist with dissolved organic matter (DOM), fulvic acid (FA), and other humic substances, and coexisting organic components can affect the adsorption of target pollutants. For example, high-temperature biochar (700 °C) tended to adsorb soil DOM, whereas low-temperature biochar (300 °C) tended to release its indigenous DOM [148]. These contrasting behaviors might influence the adsorption of organic pollutants that are sensitive to DOM variations, such as PAHs and highly polar antibiotics [149,150]. The effects of changes in coexisting organic components on the adsorption of target pollutants were also selective. Yang et al. found that DOM released in soil reduced the adsorption of PAHs by biochar, because the increase in DOM suppressed the hydrophobic partitioning and pore-filling mechanisms of biochar. In contrast, Hu et al. reported that KOH-activated biochar could simultaneously adsorb multiple pollutants, including nitrobenzene, phenols, and anilines, in the presence of FA [149]. This is because FA was preferentially adsorbed in mesopores, whereas the target pollutants were mainly adsorbed in micropores, and hydrogen bonding played a dominant role in the adsorption of nitrobenzene, phenols, and anilines. As a result, FA caused only

about 5% competitive inhibition in the system [130]. Kah et al. reached a similar conclusion in their study on the effect of soil DOM on pyrene sorption [151]. Therefore, the influence of coexisting organic matter on the adsorption of target pollutants generally depends on the molecular size, polarity, and hydrophobicity of the target pollutants, as well as on the pore size distribution of biochar. It is worth noting that the adsorption performance of biochar observed in single-component systems cannot be directly applied to practical soil studies involving multi-component coexistence. Therefore, greater attention should be paid to the pore size distribution of biochar and to the interactions among biochar, coexisting organic matter, and target pollutants.

### 6.3. Heavy Metal–Organic Pollutant Coexisting Systems

In systems co-contaminated with heavy metals and organic pollutants, the remediation behavior of biochar and the underlying influencing factors are more complex, because heavy metals and organic pollutants can interact with each other, thereby altering their mobility, bioavailability, and ecological toxicity in soil [152]. Recent studies have mostly focused on how biochar acts together with microbial communities or plants in such co-contaminated systems. For example, Zhang et al. investigated a soil environment co-contaminated with Cd(II), Zn(II), oxytetracycline, and enrofloxacin using waste fungus chaff-based biochar in combination with the antibiotic-degrading bacterium *Herbaspirillum huttiense* HHS1. The result showed that biochar not only immobilized heavy metals and adsorbed part of the organic pollutants in the co-contaminated system, but also indirectly promoted the remediation process by alleviating the inhibitory effects of heavy metals on microorganisms for providing attachment sites for HHS1 and modifying the soil environment, including pH, total phosphorus, and microbial community structure [153]. In biochar–plant remediation strategies, biochar can also assist plant-mediated heavy metal immobilization and enhance the degradation of organic pollutants by rhizosphere microorganisms, as well as the abundance of related functional genes, rather than relying solely on its own adsorption of pollutants [152]. In practical remediation studies of heavy metal–organic co-contaminated systems, more attention should be paid to the interactions among biochar, microorganisms, plants, and coexisting pollutants, rather than focusing only on the direct effect of biochar adsorption itself.

## 7. Field Application and Economic Considerations of Biochar for Soil Remediation

Although laboratory-scale studies frequently report strong remediation performance or adsorption capacity of biochar, field conditions are different, soil is heterogeneous, contaminants are unevenly distributed, and pH and redox conditions change over time. Dissolved organic matter and ions compete for sorption sites. These factors can reduce or alter biochar performance in practice [154]. Field studies were increasing [155,156], but they were still limited. Therefore, data from batch experiments should be used with caution, and field validation is necessary before large-scale application.

### 7.1. Field-Scale Application Performance

Data from a limited number of field remediation studies show that biochar application can reduce the bioavailability of heavy metals in soil, and that this effect can persist over time. For example, Zheng et al. conducted a 4-month field experiment in severely Pb-contaminated soil with a Pb concentration of up to 118,100 mg·kg<sup>-1</sup>. CaCl<sub>2</sub>-extractable Pb decreased by 95% at the 7th day when biochar was applied at 10% *w/w* [156]. Sui et al. found that the combined amendment of biochar and silicate reduced Cd concentrations in crops by 19.5–73.7% within a two-year experiment [157]. Compared with heavy metals,

field-scale evidence for the remediation of organic pollutants by biochar remains more limited, especially under complex multi-pollutant conditions. Nevertheless, some studies have begun to fill this gap [30,41]. For example, Stefaniuk et al. found that biochar amendment reduced the bioavailable fraction of PAHs in sewage sludge-amended soils from a long-term field study [158]. More recently, a study on a site co-contaminated with petroleum hydrocarbons and Cu reported that the combined use of biochar, microorganisms, and plants achieved up to 90% removal of C > 12 hydrocarbons [159].

However, unlike short-term adsorption studies conducted under laboratory conditions, the remediation performance of biochar in field trials is influenced by soil physicochemical properties, including pH, cation exchange capacity (CEC), and soil organic matter (SOM), as well as by biochar application rate. It might also be affected by biological factors in soil, such as soil fauna, microbial activity, and plant roots [160]. In addition, field aging can weaken the immediate improvement effect of biochar. Castaldi et al. found in a Mediterranean wheat field that soil pH increased from 5.23 to 6.27 within 3 months after applying biochar at 3 kg·m<sup>-2</sup>. However, soil pH declined to 5.34 after 14 months [155]. This decline might be attributed to leaching and consumption of alkalinity (e.g., ash-derived carbonates), soil buffering, and acidifying biogeochemical processes during field aging, but quantitative partitioning of these drivers remains limited in field trials.

In addition, excessive biochar application might produce adverse effects. Lima et al. found that biochars produced at 500 °C and 700 °C could effectively reduce As, Pb, and Zn contents in a maize field, but seed germination was inhibited when the biochar application rate reached 5% *w/w* [161]. Other studies have also shown that biochar application might affect soil enzyme activity [155,162]. Moreover, biochar itself may contain PAHs, dioxins and VOCs, which might cause negative environmental effects [163,164], in addition to a series of still unclear potential impacts on soil animals and plants. Thus early-stage assessment of the risk threshold for biochar application is necessary.

### 7.2. Economic Feasibility

The economic feasibility of biochar as a remediation material is usually evaluated by considering three aspects: biochar production cost, transportation and application cost, and remediation benefit relative to alternative costs. Previous studies have shown that the minimum selling price of biochar produced by conventional pyrolysis ranges from 506 to 1002 \$·t<sup>-1</sup> [165]. Therefore, the remediation cost in practical studies is closely related to the production process, application rate and expected benefits. For example, Liao et al. evaluated remediation cost using an aging model and found that the selected rice husk biochar produced at 650 °C reduced cost by 56.5% compared with conventional bamboo biochar [166]. Therefore, field studies on biochar remediation should consider contamination level, target risk threshold, recommended application rate and expected cost range, so that a feasible strategy can be developed with both economic practicality and maximum remediation performance.

### 7.3. Practical Challenges and Future Perspectives

For field trials and long-term studies, biochar remediation still faces three key challenges.

- (i) Environmental factors such as acid rain, flooding, DOM, and fluctuations in pH and oxidation-reduction reactions might weaken the remediation effect of biochar and even increase the risk of desorption under real field conditions. Therefore, it is necessary to provide evidence of contaminant desorption or remobilization in related studies.
- (ii) High biochar input can improve remediation efficiency, but it might also inhibit crop growth or introduce new pollution risks. Therefore, application dose and the ecological side effects of biochar should be evaluated before field trials.

- (iii) Field studies should include remediation cost estimation. The economic and environmental advantages of biochar can be better realized by balancing remediation cost and remediation performance.

Therefore, future studies are recommended to focus on three aspects. (1) A unified evaluation system should be established to cover short-term adsorption performance, medium-term aging evolution, and long-term re-release risk, with a comparable indicator framework across different studies. (2) Continuous cross-season validation should be carried out at typical contaminated sites. Such studies should jointly assess contaminant bioavailability, leaching risk and ecological effects, and then propose application rates matched to contamination level, together with recommended risk and cost ranges. (3) Material design should be coupled with techno-economic evaluation. Aging processes and stabilization thresholds should be incorporated into cost accounting and process optimization, so as to provide more reliable decision support for the large-scale application of biochar remediation technologies.

## 8. Conclusions and Outlook

Biochar, as an environmentally friendly material for soil pollutant remediation, has shown considerable potential in the remediation of both heavy metals and organic pollutants. Its remediation performance was not determined by a single factor, but was jointly influenced by feedstock source, preparation method, and modification strategy. This review systematically summarized different modification types of biochar by pore structure, surface functional groups, surface charge and mineral components, which could promote electrostatic adsorption, ion exchange, surface complexation, precipitation and redox transformation of heavy metals, as well as  $\pi$ - $\pi$  interactions, electron donor-acceptor interactions, hydrogen bonding, hydrophobic partitioning and pore filling for organic pollutants. Field trials and economic considerations were also discussed. Biochar exhibited clear mechanistic differences and application specificity for different types of pollutants. Based on the above findings, the following conclusions could be drawn:

- (1) For soils contaminated with heavy metals, modified biochar with abundant mineral components, strong surface complexation capacity, or redox activity should be preferentially considered.
- (2) For soils contaminated with organic pollutants, greater attention should be paid to the aromaticity, pore structure, and surface polarity of biochar.
- (3) Field application should not be judged solely on the basis of laboratory adsorption results. Soil type, contamination level, application rate, aging effects, potential ecological risks, and economic feasibility should also be comprehensively considered to achieve a balance between remediation performance and safe agricultural use.

Future applications of biochar in soil remediation still need to focus on the following aspects:

- (i) The synergistic or competitive remediation mechanism of biochar needs to be investigated in multiple pollutant system.
- (ii) Long-term field trials are needed to investigate the effects of biochar aging on the stability of remediation performance and the risk of pollutant re-release.
- (iii) A comparable standardized evaluation system is needed to assess remediation performance, environmental risk, and cost-effectiveness across different studies.
- (iv) Incorporating economic evaluation needs to be added into experimental designs to provide more reliable theoretical support for confirming the potential of large-scale application of biochar in contaminated agricultural soils.

**Author Contributions:** W.Z.: Investigation, Writing—original draft; Z.Z.: Investigation, Resources, Supervision; Z.D.: Writing—review and editing, Supervision. All authors have read and agreed to the published version of the manuscript.

**Funding:** This study was supported by the Key-Area Research and Development Program of Guangdong Province (No. 2023B0202060001), Yunfu Modern Agriculture Industry Cluster Innovation and Entrepreneurship Talent Project: Innovative and Entrepreneurial Team for Pig Manure Disposal and Resource Utilization Development (YF2024NYRC04), Innovation Team Project for Ordinary Universities in Guangdong Province (No. 2024KCXTD007), Open Research Fund Program of Shandong Provincial Key Laboratory of Eco-Environmental Science for Yellow River Delta (2025KFJJ08), Guangdong Province’s “Millions of Projects” Rural Science and Technology Special Envoy Project (KTP20240179).

**Data Availability Statement:** The data that support the findings of this study are available from the corresponding author upon reasonable request.

**Conflicts of Interest:** Author Weijian Zhang and Zeng-Hui Diao were employed by the company Guangdong Woye Fertilizer Industry Co., Ltd. The remaining author declares that the research was conducted in the absence of any commercial or financial relationships that could be construed as a potential conflict of interest.

## Abbreviations

The following abbreviations are used in this manuscript:

FA	Fulvic acid
EDA	Electron donor–acceptor
ATZ	Atrazine
OTC	Oxytetracycline
PAHs	Polycyclic aromatic hydrocarbons
PFAS	Per- and polyfluoroalkyl substances
PFOS	Perfluorooctane sulfonic acid
pHpzc	Zero charge point
OPFRs	Organic phosphate flame retardants

## References

1. Wang, S.Y.; Wang, L.Q.; Liao, X.Y.; Zhou, G.J.; Huan, Y.Z.; Li, S.; Liang, T. Impact of residential density on heavy metal mobilization in urban soils: Human activity patterns and eco-health risks in the Beijing-Tianjin-Hebei region. *Ecotoxicol. Environ. Saf.* **2025**, *302*, 118559. [[CrossRef](#)] [[PubMed](#)]
2. Zhang, R.H.; Zhang, Z.W.; Yang, J.X.; Zhang, X.; Liu, S.S.; Jin, J.C.; Liu, G.W.; Shan, C.Q.; Li, J.; Tang, J.H. Levels and associated potential ecological risks of heavy metals in surface sediments from wetlands in the western Yellow River Delta. *Reg. Stud. Mar. Sci.* **2026**, *93*, 104653. [[CrossRef](#)]
3. Zhang, Z.W.; Zhang, T.R.; Yu, W.H.; Xu, J.K.; Li, J.L.; Wu, T.; Liu, S.Z.; Wang, H.Y.; Wang, Y.X.; Shang, S.; et al. Heavy metal contamination in sediments from wetlands invaded by *Spartina alterniflora* in the Yellow River Delta. *Toxics* **2022**, *10*, 374. [[CrossRef](#)]
4. Aponte, H.; Meli, P.; Butler, B.; Paolini, J.; Matus, F.; Merino, C.; Cornejo, P.; Kuzyakov, Y. Meta-analysis of heavy metal effects on soil enzyme activities. *Sci. Total Environ.* **2020**, *737*, 139744. [[CrossRef](#)] [[PubMed](#)]
5. Wang, Y.P.; Shi, J.Y.; Wang, H.; Lin, Q.; Chen, X.; Chen, Y. The influence of soil heavy metals pollution on soil microbial biomass, enzyme activity, and community composition near a copper smelter. *Ecotoxicol. Environ. Saf.* **2007**, *67*, 75–81. [[CrossRef](#)]
6. Xie, Y.X.; Fan, J.B.; Zhu, W.X.; Amombo, E.; Lou, Y.; Chen, L.; Fu, J. Effect of Heavy Metals Pollution on Soil Microbial Diversity and Bermudagrass Genetic Variation. *Front. Plant Sci.* **2016**, *7*, 755. [[CrossRef](#)]
7. Hou, D.; O’Connor, D.; Igalavithana, A.D.; Alessi, D.S.; Luo, J.; Tsang, D.C.W.; Sparks, D.L.; Yamauchi, Y.; Rinklebe, J.; Ok, Y.S. Metal contamination and bioremediation of agricultural soils for food safety and sustainability. *Nat. Rev. Earth Environ.* **2020**, *1*, 366–381. [[CrossRef](#)]
8. Wang, M.M.; Zheng, X.H.; Oba, B.T.; Lin, Y.B.; Shen, C.B.; Huang, X.; Yang, F.X.; Xiao, Q.; Ding, Y.Z. Innovations in nanomaterials for remediation of heavy metal–polluted soil: Advances, mechanistic insights, and future prospects. *Nano Mater. Sci.* **2026**, *8*, 11–35. [[CrossRef](#)]

9. Yang, C.P.; Zhang, Z.W.; Liu, Y.; Shan, B.B.; Yu, W.; Li, H.X.; Sun, D.R. Heavy metal pollution and stable isotope ratios ( $\delta^{13}\text{C}$  and  $\delta^{15}\text{N}$ ) in marine organisms from the Northern Beibu Gulf, South China Sea. *Mar. Pollut. Bull.* **2021**, *166*, 112230. [[CrossRef](#)]
10. Yang, C.P.; Liu, Y.; Shan, B.B.; Xu, J.; Yu, W.; Sun, D.R.; Zhang, Z.W. Heavy metal concentrations and associated health risks in edible tissues of marine nekton from the outer Pearl River Estuary, South China Sea. *Environ. Sci. Pollut. Res.* **2021**, *28*, 2108–2118. [[CrossRef](#)]
11. Ren, J.Y.; Liu, S.J.; Zhang, Q.; Zhang, Z.W.; Shang, S. Effects of cadmium exposure on haemocyte immune function of clam *Ruditapes philippinarum* at different temperatures. *Mar. Environ. Res.* **2024**, *195*, 106375. [[CrossRef](#)]
12. Feyisa, G.; Mekassa, B.; Merga, L.B. Human health risks of heavy metals contamination of a water-soil-vegetables farmland system in Toke Kutaye of West Shewa, Ethiopia. *Toxicol. Rep.* **2025**, *14*, 102061. [[CrossRef](#)]
13. Pan, Z.W.; Gong, T.Y.; Liang, P. Heavy metal exposure and cardiovascular disease. *Circ. Res.* **2024**, *134*, 1160–1178. [[CrossRef](#)]
14. Botsou, F.; Sungur, A.; Kelepertzis, E.; Soylak, M. Insights into the chemical partitioning of trace metals in roadside and off-road agricultural soils along two major highways in Attica's region. *Greece. Ecotoxicol. Environ. Saf.* **2016**, *132*, 101–110. [[CrossRef](#)]
15. Zhang, Z.W.; Tong, X.; Xing, Y.; Ma, J.Y.; Jiang, R.J.; Sun, Y.X.; Li, J.L.; Li, X.P.; Wu, T.; Xie, W.J. Polybrominated diphenyl ethers, decabromodiphenyl ethane and dechlorane plus in aquatic products from the Yellow River Delta, China. *Mar. Pollut. Bull.* **2020**, *161*, 111733. [[CrossRef](#)] [[PubMed](#)]
16. Zhang, Z.W.; Pei, N.C.; Sun, Y.X.; Li, J.L.; Li, X.P.; Yu, S.; Xu, X.R.; Hu, Y.X.; Mai, B.X. Halogenated organic pollutants in sediments and organisms from mangrove wetlands of the Jiulong River Estuary, South China. *Environ. Res.* **2019**, *171*, 145–152. [[CrossRef](#)] [[PubMed](#)]
17. Hu, Y.X.; Li, Z.R.; Xiong, J.J.; Zhang, Z.W.; Yuan, J.X.; Tang, Y.; Jin, T.; Li, H.W.; Wu, S.J. Occurrence and ecological risks of brominated flame retardants and dechlorane plus in sediments from the Pearl River Estuary and Daya Bay, South China. *Mar. Pollut. Bull.* **2022**, *185*, 114182. [[CrossRef](#)]
18. Cai, J.; Zheng, P.; Qaisar, M.; Zhang, J.Q. Elemental sulfur recovery of biological sulfide removal process from wastewater: A review. *Crit. Rev. Environ. Sci. Technol.* **2017**, *47*, 2079–2099. [[CrossRef](#)]
19. Li, H.W.; Zhang, Z.W.; Sun, Y.X.; Wang, W.W.; Xie, J.L.; Xie, C.M.; Hu, Y.X.; Gao, Y.L.; Xu, X.R.; Luo, X.J.; et al. Tetrabromobisphenol A and hexabromocyclododecanes in sediments and biota from two typical mangrove wetlands of South China: Distribution, bioaccumulation and biomagnification. *Sci. Total Environ.* **2021**, *750*, 141695. [[CrossRef](#)] [[PubMed](#)]
20. Yang, X.; Song, C.Z.; Ren, M.X.; Kong, Y.; Cui, X.Y. Distribution patterns and influencing factors of PFAS in soils: A meta-analysis. *Environ. Res.* **2025**, *279*, 121806. [[CrossRef](#)]
21. Khaled, O.; Ryad, L.; Eissa, F. Determination of tetracycline residues in potatoes and soil by LC-MS/MS: Method development, validation, and risk assessment. *Food Chem.* **2024**, *461*, 140841. [[CrossRef](#)]
22. Wang, K.; Chen, W.; Zhao, F.; Li, C.; Xing, X.L.; Xu, L. Occurrence and health risk assessment of phthalate ester pollution in mulched farmland soil at a national scale, China. *J. Hazard. Mater.* **2025**, *492*, 138276. [[CrossRef](#)]
23. Chen, J.; Liu, L.H.; Huang, X.; Lu, L.L. Microbial community dynamics drive soil functional recovery after in-situ gas-thermal remediation of co-contaminated soil. *J. Hazard. Mater.* **2025**, *496*, 139303. [[CrossRef](#)]
24. Hu, D.F.; Wu, Z.; Tian, Y.M.; Liu, S.Q.; Hou, P.F.; Liang, J.S.; Zhang, G.M. Ultrasonic methods for effective soil remediation. *J. Environ. Chem. Eng.* **2025**, *13*, 118160. [[CrossRef](#)]
25. Xu, H.; Zhang, P.; Liu, G.D.; Ping, Y.; Zhang, Z.Z.; Yang, Z.H.; Yang, W.C.; Yu, J.W. As, Cd and Pb contaminated soil remediation by electrochemical methods: Mechanisms, current advances and perspective. *Desalination* **2025**, *615*, 119294. [[CrossRef](#)]
26. Zhong, P.J.; Zhang, X.L.; Yu, X.; Yang, S.D.; Yang, P.P.; Li, T.; Zhao, X.D.; Li, X.J. Soil photocatalysis revisited: Unveiling potential in organic contaminant remediation. *Chem. Eng. J.* **2025**, *521*, 166992. [[CrossRef](#)]
27. Liang, C.; Yang, S.; Xing, B.; Li, C.; Yuan, F.; Wang, J.; Dong, W.; Yan, S.; Sun, Z. Review and Perspective of Sulfate Radical Based Advanced Oxidation Processes (SR AOPs) in the Remediation of Polycyclic Aromatic Hydrocarbon (PAHs) Contaminated Soil. *J. Environ. Manag.* **2025**, *390*, 126337. [[CrossRef](#)] [[PubMed](#)]
28. Xu, J.; Guan, H.; Liu, C.; Zhou, R.; Wang, J.; Zhai, X.; Chen, T.; Wang, M. Research Progress on Remediation of Petroleum Contaminated Soil by Persulfate: Existing Technologies, Degradation Pathway and Future Direction. *J. Environ. Chem. Eng.* **2025**, *13*, 116540. [[CrossRef](#)]
29. Fu, Y.; Yi, Y.; Wang, Y.; Diao, Y.; Diao, Z.; Chen, Z. A Comprehensive Review of Modified Biochar Based Advanced Oxidation Processes for Environmental Pollution Remediation: Efficiency, Mechanism, Toxicity Assessment. *J. Environ. Manag.* **2025**, *387*, 125872. [[CrossRef](#)]
30. Haider, F.U.; Wang, X.; Zulfiqar, U.; Farooq, M.; Hussain, S.; Mehmood, T.; Naveed, M.; Li, Y.; Liqun, C.; Saeed, Q.; et al. Biochar Application for Remediation of Organic Toxic Pollutants in Contaminated Soils; An Update. *Ecotoxicol. Environ. Saf.* **2022**, *248*, 114322. [[CrossRef](#)]
31. Chen, X.; Zhang, W.X.; Chen, Z.L.; Yao, X.W.; Chen, M.L.; Tong, L.Y.; Qian, W.; Guo, P.R.; Kong, L.J.; Diao, Z.H. Efficient Activation of Persulfate by Metallic Sulfide Mineral for the Efficient Removal of Pesticides: Performance, Radical Generation and Mechanism. *J. Clean. Prod.* **2023**, *421*, 138521. [[CrossRef](#)]

32. Liu, Y.; Lonappan, L.; Brar, S.K.; Yang, S. Impact of Biochar Amendment in Agricultural Soils on the Sorption, Desorption, and Degradation of Pesticides: A Review. *Sci. Total Environ.* **2018**, *645*, 60–70. [[CrossRef](#)]
33. Qian, W.; Liang, J.Y.; Zhang, W.X.; Huang, S.T.; Diao, Z.H. A Porous Biochar Supported Nanoscale Zero Valent Iron Material Highly Efficient for the Simultaneous Remediation of Cadmium and Lead Contaminated Soil. *J. Environ. Sci.* **2022**, *113*, 231–241. [[CrossRef](#)] [[PubMed](#)]
34. Dong, F.X.; Yan, L.; Zhou, X.H.; Huang, S.T.; Liang, J.Y.; Zhang, W.X.; Guo, Z.W.; Guo, P.R.; Qian, W.; Kong, L.J.; et al. Simultaneous Adsorption of Cr(VI) and Phenol by Biochar Based Iron Oxide Composites in Water: Performance, Kinetics and Mechanism. *J. Hazard. Mater.* **2021**, *416*, 125930. [[CrossRef](#)]
35. Li, Z.Y.; Tian, W.J.; Chu, M.L.; Zou, M.Y.; Zhao, J. Molecular Imprinting Functionalization of Magnetic Biochar to Adsorb Sulfamethoxazole: Mechanism, Regeneration and Targeted Adsorption. *Process Saf. Environ. Protect.* **2023**, *171*, 238–249. [[CrossRef](#)]
36. Wang, W.J.; Lin, J.X.; Shao, S.B.; Chen, H.J.; Dai, J.W.; Yang, Y. Enhanced Adsorption of Benzo(a)Pyrene in Soil by Porous Biochar: Adsorption Kinetics, Thermodynamics, and Mechanisms. *J. Environ. Chem. Eng.* **2023**, *11*, 109002. [[CrossRef](#)]
37. Meng, Z.W.; Huang, S.; Zhao, Q.; Xin, L. Respective Evolution of Soil and Biochar on Competitive Adsorption Mechanisms for Cd(II), Ni(II), and Cu(II) after 2 Year Natural Ageing. *J. Hazard. Mater.* **2024**, *469*, 133938. [[CrossRef](#)]
38. Sohi, S.P.; Krull, E.; Lopez-Capel, E.; Bol, R. A review of biochar and its use and function in soil. *Adv. Agron.* **2010**, *105*, 47–82.
39. Ahmad, M.; Rajapaksha, A.U.; Lim, J.E.; Zhang, M.; Bolan, N.; Mohan, D.; Vithanage, M.; Lee, S.S.; Ok, Y.S. Biochar as a sorbent for contaminant management in soil and water: A review. *Chemosphere* **2014**, *99*, 19–33. [[CrossRef](#)]
40. He, L.; Zhong, H.; Liu, G.; Dai, Z.; Brookes, P.C.; Xu, J. Remediation of heavy metal contaminated soils by biochar: Mechanisms, potential risks and applications in China. *Environ. Pollut.* **2019**, *252*, 846–855. [[CrossRef](#)] [[PubMed](#)]
41. Xiang, L.; Harindintwali, J.D.; Wang, F.; Redmile-Gordon, M.; Chang, S.X.; Fu, Y.; He, C.; Muhoza, B.; Brahusi, F.; Bolan, N.; et al. Integrating Biochar, Bacteria, and Plants for Sustainable Remediation of Soils Contaminated with Organic Pollutants. *Environ. Sci. Technol.* **2022**, *56*, 16546–16566. [[CrossRef](#)] [[PubMed](#)]
42. Lyu, H.H.; Cheng, K.; He, L.L.; Yang, S.M.; Liu, Y.X.; You, L.C.; Wang, Y.Y. Efficiency of Talcum Biochars in Immobilization of Heavy Metals and Promotion of the Growth of Brassica Chinensis in Contaminated Agricultural Soil. *Plant Stress* **2025**, *16*, 100836. [[CrossRef](#)]
43. Irshad, M.K.; Lee, J.C.; Aqeel, M.; Javed, W.; Noman, A.; Lam, S.S.; Naggar, A.E.; Niazi, N.K.; Lee, H.H.; Ibrahim, M.; et al. Efficacy of Fe Mg Bimetallic Biochar in Stabilization of Multiple Heavy Metals Contaminated Soil and Attenuation of Toxicity in Spinach (*Spinacia oleracea* L.). *Chemosphere* **2024**, *364*, 143184. [[CrossRef](#)]
44. Cai, X.X.; Luo, X.S.; Yuan, Y.; Li, J.B.; Yu, Z.; Zhou, S.G. Stimulation of Phenanthrene and Biphenyl Degradation by Biochar Conducted Long Distance Electron Transfer in Soil Bioelectrochemical Systems. *Sci. Total Environ.* **2021**, *797*, 149124. [[CrossRef](#)]
45. Zhang, W.X.; Chen, X.; Xiao, G.S.; Liang, J.Y.; Kong, L.J.; Yao, X.W.; Diao, Z.H. A Novel Pigeon Waste Based Biochar Composite for the Removal of Heavy Metal and Organic Compound: Performance, Products and Mechanism. *A-Physicochem. Eng. Asp.* **2023**, *666*, 131277. [[CrossRef](#)]
46. Chen, X.; Yao, X.W.; Diao, Y.; Liu, H.; Chen, M.L.; Feng, N.J.; Qian, W.; Zhou, X.H.; Guo, P.R.; Kong, L.J.; et al. Simultaneous Removal of Triadimefon and Dinotefuran by a New Biochar Based Magnesium Oxide Composite in Water: Performances and Mechanism. *Sep. Purif. Technol.* **2024**, *336*, 126213. [[CrossRef](#)]
47. Diao, Z.H.; Zhang, W.X.; Liang, J.Y.; Huang, S.T.; Dong, F.X.; Yan, L.; Qian, W.; Chu, W. Removal of Herbicide Atrazine by a Novel Biochar Supported Zero Valent Iron Coupling with Peroxymonosulfate Process from Soil: Synergistic Effect and Mechanism. *Chem. Eng. J.* **2021**, *409*, 127684. [[CrossRef](#)]
48. Yao, X.W.; Chen, X.; Chen, M.L.; Feng, N.J.; Tong, L.Y.; Yi, Y.Q.; Qian, W.; Diao, Z.H. Removal of Pesticide Acetamiprid Using KOH Activated Biochar Derived from Crayfish Shell: Behavior and Mechanism. *Process Saf. Environ. Prot.* **2024**, *186*, 808–818. [[CrossRef](#)]
49. Liang, J.Y.; Zhang, W.X.; Yao, X.W.; Chen, M.L.; Chen, X.; Kong, L.J.; Diao, Z.H. New Insights into Co Adsorption of Cr<sup>6+</sup> and Chlortetracycline by a New Fruit Peel Based Biochar Composite from Water: Behavior and Mechanism. *Colloids Surf. A-Physicochem. Eng. Asp.* **2023**, *672*, 131764.
50. Huang, S.T.; Lei, Y.Q.; Guo, P.R.; Zhang, W.X.; Liang, J.Y.; Chen, X.; Xu, J.W.; Diao, Z.H. Degradation of Levofloxacin by a Green Zero Valent Iron Loaded Carbon Composite Activating Peroxydisulfate System: Reactivity, Products and Mechanism. *Chemosphere* **2023**, *340*, 139899. [[CrossRef](#)]
51. Yan, L.; Dong, F.X.; Lin, X.; Zhou, X.H.; Kong, L.J.; Chu, W.; Diao, Z.H. Insights into the Removal of Cr(VI) by a Biochar–Iron Composite from Aqueous Solution: Reactivity, Kinetics and Mechanism. *Environ. Technol. Innov.* **2021**, *24*, 102057. [[CrossRef](#)]
52. Yan, L.; Dong, F.X.; Li, Y.; Guo, P.R.; Kong, L.J.; Chu, W.; Diao, Z.H. Synchronous Removal of Cr(VI) and Phosphates by a Novel Crayfish Shell Biochar Fe Composite from Aqueous Solution: Reactivity and Mechanism. *J. Environ. Chem. Eng.* **2022**, *10*, 107396. [[CrossRef](#)]

53. Song, Y.B.; Tan, J.W.; Jin, M.Y.; Liu, Z.; Zhu, J.F.; El Sayed, M.E.A.; Abdelhafeez, I.A.; Zhang, Y.L.; Shen, Z. Effect of Pyrolysis Temperature and Heating Rate on the Physicochemical Properties of Alkali Lignin Derived Biochar: A Comparative Study of Fast and Slow Pyrolysis. *J. Anal. Appl. Pyrolysis* **2025**, *191*, 107236. [CrossRef]
54. Leng, L.J.; Huang, H.J. An Overview of the Effect of Pyrolysis Process Parameters on Biochar Stability. *Bioresour. Technol.* **2018**, *270*, 627–642. [CrossRef] [PubMed]
55. Dhyani, V.; Bhaskar, T. A comprehensive review on the pyrolysis of lignocellulosic biomass. *Renew. Sustain. Energy Rev.* **2018**, *90*, 223–247. [CrossRef]
56. Al-Rumaihi, A.; Shahbaz, M.; McKay, G.; Mackey, H.; Al-Ansari, T. A review of pyrolysis technologies and feedstock: A blending approach for plastic and biomass towards optimum biochar yield. *Renew. Sustain. Energy Rev.* **2022**, *167*, 112715. [CrossRef]
57. Kan, T.; Strezov, V.; Evans, T.J. Lignocellulosic biomass pyrolysis: A review of product properties and effects of pyrolysis parameters. *Renew. Sustain. Energy Rev.* **2016**, *57*, 1126–1140. [CrossRef]
58. Foong, S.Y.; Liew, R.K.; Yang, Y.; Cheng, Y.W.; Yek, P.N.Y.; Wan Mahari, W.A.; Lee, X.Y.; Han, C.S.; Vo, D.V.N.; Van Le, Q.; et al. Valorization of Biomass Waste to Engineered Activated Biochar by Microwave Pyrolysis: Progress, Challenges, and Future Directions. *Chem. Eng. J.* **2020**, *389*, 124401. [CrossRef]
59. Zhang, Y.; Wang, T.; Ma, L.; Peng, P.; Min, M.; Cheng, Y.; Anderson, E.; Zhou, N.; Fan, L.; Liu, C. Effects of feedstock characteristics on microwave-assisted pyrolysis: A review. *Bioresour. Technol.* **2017**, *230*, 143–151. [CrossRef]
60. Ge, S.; Yek, P.N.Y.; Cheng, Y.W.; Xia, C.; Mahari, W.A.W.; Liew, R.K.; Peng, W.; Yuan, T.-Q.; Tabatabaei, M.; Aghbashlo, M.; et al. Progress in microwave pyrolysis conversion of agricultural waste to value-added biofuels: A batch to continuous approach. *Renew. Sustain. Energy Rev.* **2021**, *135*, 110148. [CrossRef]
61. Qiu, B.; Wang, Y.; Zhang, D.; Chu, H. Microwave-assisted pyrolysis of biomass to high-value products: Factors assessment, mechanism analysis, and critical issues proposal. *Chem. Eng. J.* **2024**, *498*, 155362. [CrossRef]
62. Jang, E.S.; Ryu, D.Y.; Kim, D. Hydrothermal Carbonization Improves the Quality of Biochar Derived from Livestock Manure by Removing Inorganic Matter. *Chemosphere* **2022**, *305*, 135391. [CrossRef]
63. Wang, T.; Zhai, Y.; Zhu, Y.; Li, C.; Zeng, G. A review of the hydrothermal carbonization of biomass waste for hydrochar formation: Process conditions, fundamentals, and physicochemical properties. *Renew. Sustain. Energy Rev.* **2018**, *90*, 223–247. [CrossRef]
64. Czerwińska, K.; Śliz, M.; Wilk, M. Hydrothermal carbonization process: Fundamentals, main parameter characteristics and possible applications including an effective method of SARS-CoV-2 mitigation in sewage sludge. A review. *Renew. Sustain. Energy Rev.* **2022**, *154*, 111873. [CrossRef]
65. Aragón-Briceño, C.I.; Pozarlik, A.K.; Bramer, E.A.; Niedzwiecki, L.; Pawlak-Kruczek, H.; Brem, G. Hydrothermal carbonization of wet biomass from nitrogen and phosphorus approach: A review. *Renew. Energy* **2021**, *171*, 401–415. [CrossRef]
66. Zhi, Y.; Xu, D.; Jiang, G.; Yang, W.; Chen, Z.; Duan, P.; Zhang, J. A review of hydrothermal carbonization of municipal sludge: Process conditions, physicochemical properties, methods coupling, energy balances and life cycle analyses. *Fuel Process. Technol.* **2024**, *254*, 107943. [CrossRef]
67. Wang, X.; Guo, Q.; Wang, X.; Jia, Y.; Chen, W.; Zhang, Q.; Yuan, J. Effect of biochars on the immobilization and form transformation of cadmium in iron-rich contaminated soil. *Ecotoxicol. Environ. Saf.* **2024**, *272*, 116045. [CrossRef]
68. Zhao, X.; Miao, R.; Guo, M.; Shang, X.; Zhou, Y.; Zhu, J. Biochar enhanced polycyclic aromatic hydrocarbons degradation in soil planted with ryegrass: Bacterial community and degradation gene expression mechanisms. *Sci. Total Environ.* **2022**, *838*, 156076. [CrossRef]
69. Shao, J.G.; Zhang, J.J.; Zhang, X.; Feng, Y.; Zhang, H.; Zhang, S.H.; Chen, H. Enhance SO<sub>2</sub> Adsorption Performance of Biochar Modified by CO<sub>2</sub> Activation and Amine Impregnation. *Fuel* **2018**, *224*, 138–146. [CrossRef]
70. Shim, T.; Yoo, J.; Ryu, C.; Park, Y.-K.; Jung, J. Effect of steam activation of biochar produced from a giant Miscanthus on copper sorption and toxicity. *Bioresour. Technol.* **2015**, *197*, 85–90. [CrossRef]
71. Yao, F.; Ye, G.Z.; Peng, W.X.; Zhao, G.Y.; Wang, X.H.; Wang, Y.Q.; Zhu, W.F.; Jiao, Y.J.; Huang, H.M.; Ye, D.Q. Preparation of Activated Biochar with Adjustable Pore Structure by Hydrothermal Carbonization for Efficient Adsorption of VOCs and Its Practical Application Prospects. *J. Environ. Chem. Eng.* **2023**, *11*, 109611. [CrossRef]
72. Liu, L.; Li, Y.; Fan, S. Preparation of KOH and H<sub>3</sub>PO<sub>4</sub> Modified Biochar and Its Application in Methylene Blue Removal from Aqueous Solution. *Processes* **2019**, *7*, 891. [CrossRef]
73. Danesh, P.; Prussi, M.; Salimbeni, A.; Negro, V.; Chiaramonti, D. Review on Biochar Upgrading Methods for Its Application in Thermochemical Conversion Processes and Critical Materials Recovery. *Sustainability* **2025**, *17*, 10194. [CrossRef]
74. Zhang, J.J.; Shao, J.G.; Jin, Q.Z.; Zhang, X.; Yang, H.P.; Chen, Y.Q.; Zhang, S.H.; Chen, H.P. Effect of Deashing on Activation Process and Lead Adsorption Capacities of Sludge Based Biochar. *Sci. Total Environ.* **2020**, *716*, 137016. [CrossRef]
75. Qu, J.; Wang, Y.; Tian, X.; Jiang, Z.; Deng, F.; Tao, Y.; Jiang, Q.; Wang, L.; Zhang, Y. KOH-activated porous biochar with high specific surface area for adsorptive removal of chromium (VI) and naphthalene from water: Affecting factors, mechanisms and reusability exploration. *J. Hazard. Mater.* **2021**, *401*, 123292. [CrossRef] [PubMed]

76. Zhang, R.L.; Zhang, X.Y.; Du, S.; Zhang, R.R.; Gao, J.Y.; Zhang, Y.J.; Liu, J.P. Investigation of the Degradation Mechanism of Dibutyl Phthalate in Soil Using Alkali-Modified Biochar and Persulfate Systems. *Water Air Soil Pollut.* **2026**, *237*, 751. [[CrossRef](#)]
77. Sanford, J.R.; Larson, R.A.; Runge, T. Nitrate Sorption to Biochar Following Chemical Oxidation. *Sci. Total Environ.* **2019**, *669*, 938–947. [[CrossRef](#)] [[PubMed](#)]
78. Zhang, W.; Cho, Y.; Vithanage, M.; Shaheen, S.M.; Rinklebe, J.; Alessi, D.S.; Hou, C.H.; Hashimoto, Y.; Withana, P.A.; Ok, Y.S. Arsenic Removal from Water and Soils Using Pristine and Modified Biochars. *Biochar* **2022**, *4*, 55. [[CrossRef](#)]
79. Akin, S.S.; Kir, A.B.; Kazanc, F. Impact of Nitrogen and Alkali Dopants on Pore Architecture and Surface Functionalities of Biochar in One Step CO<sub>2</sub> Pyrolysis. *J. Anal. Appl. Pyrolysis* **2025**, *186*, 106962. [[CrossRef](#)]
80. Jia, Z.H.; Guo, H.L.; Han, Z.L.; Zhao, C.L.; Zhang, J.J.; Cheng, Z.Q. Synergistic Sulfur Nitrogen Co Doping in Micro Biochar: Dynamic Redox Mechanisms for Enhanced Multipollutant Co Adsorption. *J. Environ. Chem. Eng.* **2025**, *13*, 118314. [[CrossRef](#)]
81. Lin, X.N.; Chen, X.Y.; Fu, P.; Tang, B.B.; Bi, D.M. Highly Efficient Production of Monocyclic Aromatics from Catalytic Co Pyrolysis of Biomass and Plastic with Nitrogen Doped Activated Carbon Catalyst. *Chem. Eng. J.* **2023**, *474*, 145783. [[CrossRef](#)]
82. He, D.W.; Wang, Q.H.; Mu, J. Conversion of Waste Cork to N Doped Porous Carbons by Urea Assisted Hydrothermal Method for Enhanced VOC Capture. *Waste Manag.* **2024**, *175*, 191–203. [[CrossRef](#)]
83. Zhou, C.L.; Song, X.; Wang, Y.W.; Wang, H.; Ge, S.F. The Sorption and Short Term Immobilization of Lead and Cadmium by Nano Hydroxyapatite/Biochar in Aqueous Solution and Soil. *Chemosphere* **2022**, *286*, 131810. [[CrossRef](#)] [[PubMed](#)]
84. Dong, W.; Xing, J.; Chen, Q.; Huang, Y.; Wu, M.; Yi, P.; Pan, B.; Xing, B.S. Hydrogen Bonds between the Oxygen Containing Functional Groups of Biochar and Organic Contaminants Significantly Enhance Sorption Affinity. *Chem. Eng. J.* **2024**, *499*, 156654. [[CrossRef](#)]
85. Wang, L.; Ok, Y.S.; Tsang, D.C.W.; Alessi, D.S.; Rinklebe, J.; Wang, H.; Mašek, O.; Hou, R.; O'Connor, D.; Hou, D. New trends in biochar pyrolysis and modification strategies: Feedstock, pyrolysis conditions, sustainability concerns and implications for soil amendment. *Soil Use Manag.* **2020**, *36*, 358–386. [[CrossRef](#)]
86. Tao, J.H.; Chen, D.; Wu, S.F.; Zhang, Q.; Xiao, W.D.; Zhao, S.P.; Ye, X.Z.; Chu, T.F. The Comprehensive Effects of Biochar Amendments on Soil Organic Carbon Accumulation, Soil Acidification Amelioration and Heavy Metal Availability in the Soil–Rice System. *Agronomy* **2024**, *14*, 2498. [[CrossRef](#)]
87. Gu, X.; Guo, P.H.; Li, Z.S.; Xu, X.; Cao, Y.N.; Yang, G.E.; Kuang, C.T.; Li, X.G.; Qing, Y.; Wu, Y.Q. A Multifunctional Coconut Shell Biochar Modified by Titanium Dioxide for Heavy Metal Removal in Water/Soil and Tetracycline Degradation. *J. Clean. Prod.* **2024**, *482*, 144192. [[CrossRef](#)]
88. Wu, Y.J.; Chen, B.L. Effect of Fulvic Acid Coating on Biochar Surface Structure and Sorption Properties towards 4 Chlorophenol. *Sci. Total Environ.* **2019**, *691*, 595–604. [[CrossRef](#)]
89. Hassan, M.; Liu, Y.J.; Naidu, R.; Du, J.H.; Qi, F.J. Adsorption of Perfluorooctane Sulfonate (PFOS) onto Metal Oxides Modified Biochar. *Environ. Technol. Innov.* **2020**, *19*, 100816. [[CrossRef](#)]
90. Yang, X.; Deng, D.; Liu, Z.; Ke, W.; Xue, S.; Zhu, F. Pb/As Simultaneous Removal from Soil Leachate of Pb/Zn Smelting Sites by Magnetic Biochar. *J. Environ. Manag.* **2024**, *365*, 121526. [[CrossRef](#)] [[PubMed](#)]
91. Liang, M.; Lu, L.; Zhang, Q.; Li, J.; Qiao, M.; Wu, Z. Time Scale Effect of Magnetic Ferric Oxide Modified Biochar in Situ Remediation of Arsenic Contaminated Paddy Soil. *Environ. Technol. Innov.* **2024**, *35*, 103727. [[CrossRef](#)]
92. Zhang, Q.; Liang, M.; Li, J.; Zhang, J.; Zhang, X.; Wang, D. Sustainable in Situ Arsenic Immobilization in Paddy Soils Using Magnetic Biochar and the Role of Microbial Functional Genes. *J. Environ. Manag.* **2025**, *392*, 126916. [[CrossRef](#)]
93. Hashemi, E.; Norouzi, M.M.; Sadeghi Kiakhani, M. Magnetic Biochar as a Revolutionizing Approach for Diverse Dye Pollutants Elimination: A Comprehensive Review. *Environ. Res.* **2024**, *261*, 119548. [[CrossRef](#)] [[PubMed](#)]
94. Tang, Z.L.; Liang, M.N.; Ding, Y.M.; Liu, C.M.; Zhang, Q.; Wang, D.Q.; Zhang, X.H. Fe<sub>3</sub>O<sub>4</sub>/Mulberry Stem Biochar as a Potential Amendment for Highly Arsenic-Contaminated Paddy Soil Remediation. *Toxics* **2024**, *12*, 765. [[CrossRef](#)] [[PubMed](#)]
95. Diao, Z.H.; Du, J.J.; Jiang, D.; Kong, L.J.; Huo, W.Y.; Liu, C.M.; Wu, Q.H.; Xu, X.R. Insights into the Simultaneous Removal of Cr<sup>6+</sup> and Pb<sup>2+</sup> by a Novel Sewage Sludge Derived Biochar Immobilized Nanoscale Zero Valent Iron: Coexistence Effect and Mechanism. *Sci. Total Environ.* **2018**, *642*, 505–515. [[CrossRef](#)]
96. Diao, Z.H.; Yan, L.; Dong, F.X.; Qian, W.; Deng, Q.H.; Kong, L.J.; Yang, J.W.; Lei, Z.X.; Du, J.J.; Chu, W. Degradation of 2,4 Dichlorophenol by a Novel Iron Based System and Its Synergism with Cd(II) Immobilization in a Contaminated Soil. *Chem. Eng. J.* **2020**, *379*, 122313. [[CrossRef](#)]
97. Sun, L.J.; Gong, P.Y.; Sun, Y.F.; Qin, Q.; Song, K.; Ye, J.; Zhang, H.; Zhou, B.; Xue, Y. Modified Chicken Manure Biochar Enhanced the Adsorption for Cd<sup>2+</sup> in Aqueous and Immobilization of Cd in Contaminated Agricultural Soil. *Sci. Total Environ.* **2022**, *851*, 158252. [[CrossRef](#)] [[PubMed](#)]
98. Anum, S.; Liu, S.; Zhang, P.; Bostani, A.; Wang, X.H.; Sun, H.W. Sand Milled Nanosized N Doped Biochar for the Efficient Remediation of Pb and Cd Contaminated Soil: Preparation, Performance and Mechanism. *J. Environ. Chem. Eng.* **2024**, *12*, 114007. [[CrossRef](#)]

99. Chakma, S.; Hasan, M.; Hu, Y.L.; Rakshit, S.K.; Kang, K. Valorization of Red Mud and Biomass Waste via Pre Pyrolysis Activation for High Performance Magnetic Biochar in Heavy Metal Remediation. *Waste Manag.* **2025**, *204*, 114970. [[CrossRef](#)]
100. Kang, X.R.; Geng, N.; Li, Y.P.; He, W.; Wang, H.; Pan, H.; Yang, Q.Q.; Yang, Z.C.; Sun, Y.J.; Lou, Y.H.; et al. Biochar with KMnO<sub>4</sub> Hematite Modification Promoted Foxtail Millet Growth by Alleviating Soil Cd and Zn Biototoxicity. *J. Hazard. Mater.* **2024**, *477*, 135377. [[CrossRef](#)]
101. Qiu, Z.; Tang, J.W.; Chen, J.H.; Zhang, Q.Z. Remediation of Cadmium Contaminated Soil with Biochar Simultaneously Improves Biochar's Recalcitrance. *Environ. Pollut.* **2020**, *256*, 113436. [[CrossRef](#)] [[PubMed](#)]
102. Zhu, L.; Tong, L.; Zhao, N.; Wang, X.; Yang, X.X.; Lv, Y.Z. Key Factors and Microscopic Mechanisms Controlling Adsorption of Cadmium by Surface Oxidized and Aminated Biochars. *J. Hazard. Mater.* **2020**, *382*, 121002. [[CrossRef](#)]
103. Su, J.Z.; Guo, Z.L.; Zhang, M.Y.; Xie, Y.M.; Shi, R.; Huang, X.F.; Tuo, Y.F.; He, X.; Xiang, P. Mn Modified Bamboo Biochar Improves Soil Quality and Immobilizes Heavy Metals in Contaminated Soils. *Environ. Technol. Innov.* **2024**, *34*, 103630. [[CrossRef](#)]
104. Xiao, S.Q.; Ding, S.; Gao, W.; Qi, X. Hydroxyapatite Self Doped Biochar with MgO Modification Immobilizes Heavy Metal and Alters Soil Microbial Community. *J. Environ. Chem. Eng.* **2024**, *12*, 114283. [[CrossRef](#)]
105. Su, M.M.; Tian, H.W.; Guo, Z.C.; Luo, G.J.; Gong, X.; Li, X.E.; Yan, H.Y.; Shen, L.C.; Yang, S.J.; He, T.B.; et al. Utilization of SiO<sub>2</sub> NP Modified Biochar from Invasive Plants to Mitigate Heavy Metal Stress in *Allium Hookeri*. *Environ. Technol. Innov.* **2025**, *37*, 104041. [[CrossRef](#)]
106. Li, K.; Xu, W.; Song, H.; Bi, F.; Li, Y.; Jiang, Z.; Tao, Y.; Qu, J.; Zhang, Y. Superior reduction and immobilization of Cr(VI) in soil utilizing sulfide nanoscale zero-valent iron supported by phosphoric acid-modified biochar: Efficiency and mechanism investigation. *Sci. Total Environ.* **2024**, *907*, 168133. [[CrossRef](#)]
107. Zhang, D.; Lin, J.; Luo, J.; Sun, S.; Zhang, X.; Ma, R.; Peng, J.; Ji, F.; Zheng, S.; Tian, Z.; et al. Rapid Immobilization of Arsenic in Contaminated Soils by Microwave Irradiation Combined with Magnetic Biochar: Microwave-Induced Electron Transfer for Oxidation and Immobilization of Arsenic (III). *Sci. Total Environ.* **2024**, *919*, 170916. [[CrossRef](#)] [[PubMed](#)]
108. Xu, R.K.; Xiao, S.C.; Yuan, J.H.; Zhao, A.Z. Adsorption of Methyl Violet from Aqueous Solutions by the Biochars Derived from Crop Residues. *Bioresour. Technol.* **2011**, *102*, 10293–10298. [[CrossRef](#)] [[PubMed](#)]
109. Qiu, Y.; Zheng, Z.Z.; Zhou, Z.L.; Sheng, G.D. Effectiveness and Mechanisms of Dye Adsorption on a Straw Based Biochar. *Bioresour. Technol.* **2009**, *100*, 5348–5351. [[CrossRef](#)]
110. Gao, L.; Li, Z.H.; Yi, W.M.; Wang, L.H.; Zhang, P.; Wan, Z.; Li, Y.F. Quantitative Contribution of Minerals and Organics in Biochar to Pb(II) Adsorption: Considering the Increase of Oxygen Containing Functional Groups. *J. Clean. Prod.* **2021**, *325*, 129328. [[CrossRef](#)]
111. Zhang, Y.H.; Zeng, H.; Dong, X.W.; Huang, H.L.; Zheng, Q.; Dai, Z.H.; Zhang, Z.W.; Li, Z.Y.; Feng, Q.M.; Xiong, S.L.; et al. In Situ Cadmium Removal from Paddy Soils by a Reusable Remediation Device and Its Health Risk Assessment in Rice. *Environ. Technol. Innov.* **2021**, *23*, 101713. [[CrossRef](#)]
112. Xin, L.; Huang, S.; Meng, Z.W.; Deng, Y.Y. Impact Mechanisms of Polyethylene Microplastic on Cd Adsorption and Passivation by KMnO<sub>4</sub> Modified Biochar in Different Soils. *Environ. Res.* **2025**, *285*, 122476. [[CrossRef](#)]
113. Meng, Z.W.; Huang, S.; Wu, J.W.; Deng, Y.Y. Adsorption, Immobilization Mechanisms and Potential Risks of Cd in Soil Biochar Microplastics System. *J. Environ. Manag.* **2025**, *392*, 126655. [[CrossRef](#)]
114. Wang, S.; Zhou, Q.; Han, X.; Wang, M.; Liu, X.; Jiang, Q.; Liu, T.; Qu, J.; Zhang, Y. Biochar-supported sulfurized nano-zero-valent iron for soil Cr(VI) immobilization: Mitigating migration and elucidating reduction mechanisms. *Chem. Eng. J.* **2026**, *527*, 171424. [[CrossRef](#)]
115. Hua, L.; Wu, C.; Zhang, H.; Cao, L.; Wei, T.; Guo, J. Biochar-Induced Changes in Soil Microbial Affect Species of Antimony in Contaminated Soils. *Chemosphere* **2021**, *263*, 127795. [[CrossRef](#)] [[PubMed](#)]
116. Yang, X.; Fan, J.; Jiang, L.; Zhu, F.; Yan, Z.; Li, X.; Jiang, P.; Li, X.; Xue, S. Using Fe/H<sub>2</sub>O<sub>2</sub>-Modified Biochar to Realize Field-Scale Sb/As Stabilization and Soil Structure Improvement in an Sb Smelting Site. *Sci. Total Environ.* **2024**, *912*, 168775. [[CrossRef](#)] [[PubMed](#)]
117. Liu, C.M.; Diao, Z.H.; Huo, W.Y.; Kong, L.J.; Du, J.J. Simultaneous Removal of Cu<sup>2+</sup> and Bisphenol A by a Novel Biochar Supported Zero Valent Iron from Aqueous Solution: Synthesis, Reactivity and Mechanism. *Environ. Pollut.* **2018**, *239*, 698–705. [[CrossRef](#)]
118. Wu, H.W.; Feng, Q.; Lu, P.; Chen, M.; Yang, H. Degradation Mechanisms of Cefotaxime Using Biochar Supported Co/Fe Bimetallic Nanoparticles. *Environ. Sci. Water Res. Technol.* **2018**, *4*, 964–975. [[CrossRef](#)]
119. Qin, J.M.; Li, J.X.; Pei, H.H.; Li, Q.H.; Cheng, D.M.; Zhou, J.; Pei, G.P.; Wang, Y.Y.; Liu, F.W. Effective Remediation and Phytotoxicity Assessment of Oxytetracycline and Cd Co Contaminated Soil Using Biochar. *Environ. Technol. Innov.* **2024**, *35*, 103649. [[CrossRef](#)]
120. Mazarji, M.; Minkina, T.; Sushkova, S.; Mandzheva, S.; Bayero, M.T.; Fedorenko, A.; Mahmoodi, N.M.; Sillanpää, M.; Bauer, T.; Soldatov, A. Metal Organic Frameworks (MIL 101) Decorated Biochar as a Highly Efficient Bio Based Composite for Immobilization of Polycyclic Aromatic Hydrocarbons and Copper in Real Contaminated Soil. *J. Environ. Chem. Eng.* **2022**, *10*, 108821. [[CrossRef](#)]
121. Feng, Z.Q.; Zhou, B.H.; Yuan, R.F.; Li, H.Q.; He, P.D.; Wang, F.; Chen, Z.B.; Chen, H.L. Biochar Derived from Different Crop Straws as Persulfate Activator for the Degradation of Sulfadiazine: Influence of Biomass Types and Systemic Cause Analysis. *Chem. Eng. J.* **2022**, *440*, 135669. [[CrossRef](#)]

122. Ke, Y.X.; Zhang, X.; Ren, Y.H.; Zhu, X.L.; Si, S.C.; Kou, B.; Zhang, Z.Y.; Wang, J.Q.; Shen, B.S. Remediation of Polycyclic Aromatic Hydrocarbons Polluted Soil by Biochar Loaded Humic Acid Activating Persulfate: Performance, Process and Mechanisms. *Bioresour. Technol.* **2024**, *399*, 130633. [[CrossRef](#)]
123. Hu, M.; Wu, W.H.; Zhou, C.K.; Zhu, H.X.; Hu, L.G.; Jiang, L.; Lin, D.H.; Yang, K. Simultaneous Adsorption of Fulvic Acid and Organic Contaminants by KOH Activated Mesoporous Biochar with Large Surface Area. *Heliyon* **2024**, *10*, e27055. [[CrossRef](#)]
124. Sørmo, E.; Silvani, L.; Bjerkli, N.; Hagemann, N.; Zimmerman, A.R.; Hale, S.E.; Hansen, C.B.; Hartnik, T.; Cornelissen, G. Stabilization of PFAS-Contaminated Soil with Activated Biochar. *Sci. Total Environ.* **2021**, *763*, 144034. [[CrossRef](#)] [[PubMed](#)]
125. Xu, T.; Lou, L.; Luo, L.; Cao, R.; Duan, D.; Chen, Y. Effect of Bamboo Biochar on Pentachlorophenol Leachability and Bioavailability in Agricultural Soil. *Sci. Total Environ.* **2012**, *414*, 727–731. [[CrossRef](#)]
126. Qu, J.; Li, Z.; Wang, S.; Lin, Q.; Zhang, Z.; Wu, Z.; Hu, Q.; Jiang, Z.; Tao, Y.; Zhang, Y. Enhanced Degradation of Atrazine from Soil with Recyclable Magnetic Carbon Based Bacterial Pellets: Performance and Mechanism. *Chem. Eng. J.* **2024**, *490*, 151662. [[CrossRef](#)]
127. Joshi, M.; Bhatt, D.; Srivastava, A. Enhanced Adsorption Efficiency through Biochar Modification: A Comprehensive Review. *Ind. Eng. Chem. Res.* **2023**, *62*, 13748–13761. [[CrossRef](#)]
128. Sun, Y.H.; Lyu, H.H.; Cheng, Z.; Wang, Y.Z.; Tang, J.C. Insight into the Mechanisms of Ball Milled Biochar Addition on Soil Tetracycline Degradation Enhancement: Physicochemical Properties and Microbial Community Structure. *Chemosphere* **2022**, *291*, 132691. [[CrossRef](#)] [[PubMed](#)]
129. Tang, W.; Zhanli, B.L.G.L.; Jing, F.Q.; Hu, T.T.; Chen, J.W. Low Temperature Pyrolytic Biochar Is a Preferred Choice for Sulfonamide Cu(II) Contaminated Soil Remediation in Tropical Climate Region. *Sci. Total Environ.* **2023**, *876*, 162792. [[CrossRef](#)]
130. Du, Z.; Huang, C.; Meng, J.; Yuan, Y.; Yin, Z.; Feng, L.; Liu, Y.; Zhang, L. Sorption of Aromatic Organophosphate Flame Retardants on Thermally and Hydrothermally Produced Biochars. *Front. Environ. Sci. Eng.* **2020**, *14*, 43. [[CrossRef](#)]
131. Newcomb, C.J.; Qafoku, N.P.; Grate, J.W.; Bailey, V.L.; De Yoreo, J.J. Developing a Molecular Picture of Soil Organic Matter–Mineral Interactions by Quantifying Organo–Mineral Binding. *Nat. Commun.* **2017**, *8*, 396. [[CrossRef](#)]
132. Yang, L.; Yang, X.; Guo, J.; Yang, Z.; Du, Y.; Lu, Q.; Zhong, G. Invasive Plant-Derived Biochar for Sustainable Bioremediation of Pesticide Contaminated Soil. *Chem. Eng. J.* **2024**, *491*, 148689. [[CrossRef](#)]
133. Zhu, H.; Liu, X.; Jiang, Y.; Zhang, M.; Lin, D.; Yang, K. Time-dependent desorption of anilines, phenols, and nitrobenzenes from biochar produced at 700 °C: Insight into desorption hysteresis. *Chem. Eng. J.* **2021**, *422*, 130584. [[CrossRef](#)]
134. Hu, M.; Wu, W.; Lin, D.; Yang, K. Adsorption of fulvic acid on mesopore-rich activated carbon with high surface area. *Sci. Total Environ.* **2022**, *838*, 155918. [[CrossRef](#)]
135. Wei, Z.; Hou, C.; Gao, Z.; Wang, L.; Yang, C.; Li, Y.; Liu, K.; Sun, Y. Preparation of biochar with developed mesoporous structure from poplar leaf activated by KHCO<sub>3</sub> and its efficient adsorption of oxytetracycline hydrochloride. *Molecules* **2023**, *28*, 3188. [[CrossRef](#)]
136. Lee, S.-C.; Kitamura, Y.; Chien, C.-C.; Cheng, C.-S.; Cheng, J.-H.; Tsai, S.-H.; Hsieh, C.-C. Development of meso- and macro-pore carbonization technology from biochar in treating the stumps of representative trees in Taiwan. *Sustainability* **2022**, *14*, 14792. [[CrossRef](#)]
137. Hao, J.; Zhang, X.; Zong, S.; Zhuo, Y.; Zhang, Y.; Wang, S.; Deng, Y.; Zhang, X.; Li, J. Biochar as a highly efficient adsorption carrier for sewage sludge-derived nutrients and biostimulants: Component fixation and mechanism. *Biochar* **2024**, *6*, 42. [[CrossRef](#)]
138. Zhang, P.; Sun, H.W.; Ren, C.; Min, L.J.; Zhang, H.M. Sorption Mechanisms of Neonicotinoids on Biochars and the Impact of Deashing Treatments on Biochar Structure and Neonicotinoids Sorption. *Environ. Pollut.* **2018**, *234*, 812–820. [[CrossRef](#)]
139. Jin, J.; Kang, M.; Sun, K.; Pan, Z.; Wu, F.; Xing, B. Properties of Biochar-Amended Soils and Their Sorption of Imidacloprid, Isoproturon, and Atrazine. *Sci. Total Environ.* **2016**, *550*, 504–513. [[CrossRef](#)]
140. Song, Y.; Wang, F.; Bian, Y.; Kengara, F.O.; Jia, M.; Xie, Z.; Jiang, X. Bioavailability Assessment of Hexachlorobenzene in Soil as Affected by Wheat Straw Biochar. *J. Hazard. Mater.* **2012**, *217–218*, 391–397. [[CrossRef](#)]
141. Song, Y.; Wang, F.; Kengara, F.O.; Yang, X.; Gu, C.; Jiang, X. Immobilization of Chlorobenzenes in Soil Using Wheat Straw Biochar. *J. Agric. Food Chem.* **2013**, *61*, 4210–4217. [[CrossRef](#)]
142. Kołtowski, M.; Hilber, I.; Bucheli, T.D.; Oleszczuk, P. Effect of Steam Activated Biochar Application to Industrially Contaminated Soils on Bioavailability of Polycyclic Aromatic Hydrocarbons and Ecotoxicity of Soils. *Sci. Total Environ.* **2016**, *566–567*, 1023–1031. [[CrossRef](#)]
143. Tang, X.-Y.; Yin, W.-M.; Yang, G.; Cui, J.-F.; Cheng, J.-H.; Yang, F.; Li, X.-Y.; Wu, C.-Y.; Zhu, S.-G. Biochar Reduces Antibiotic Transport by Altering Soil Hydrology and Enhancing Antibiotic Sorption. *J. Hazard. Mater.* **2024**, *472*, 134468. [[CrossRef](#)]
144. Chandhi, K.; Udomkun, P.; Boonupara, T.; Kaewlom, P. Enhancing Soil Health, Microbial Count, and Hydrophilic Methomyl and Hydrophobic Lambda-Cyhalothrin Remediation with Biochar and Nano-Biochar. *Sci. Rep.* **2024**, *14*, 19551. [[CrossRef](#)]
145. Liu, X.; He, Y.; Li, J.; Zheng, S.; Zhang, L.; Zhang, J.; Tang, X. Does Biochar Field Aging Reduce the Kinetic Retention for Weakly Hydrophobic Antibiotics in Purple Soil? *Biochar* **2025**, *7*, 69. [[CrossRef](#)]
146. Deng, Y.; Huang, S.; Laird, D.A.; Wang, X.; Meng, Z. Adsorption behaviour and mechanisms of cadmium and nickel on rice straw biochars in single- and binary-metal systems. *Chemosphere* **2019**, *218*, 308–318. [[CrossRef](#)]

147. Meng, Z.; Huang, S.; Wu, J.; Lin, Z. Competitive adsorption and immobilization of Cd, Ni, and Cu by biochar in unsaturated soils under single-, binary-, and ternary-metal systems. *J. Hazard. Mater.* **2023**, *451*, 131106. [[CrossRef](#)]
148. Feng, Z.; Zhu, M.; Fan, F.; Zhan, X.; Chen, C. Biochar induced changes of soil dissolved organic matter: The release and adsorption of dissolved organic matter by biochar and soil. *Sci. Total Environ.* **2021**, *798*, 149197. [[CrossRef](#)]
149. Yang, X.-H.; Song, H.; Cheng, F.; Wu, C.-H.; Tao, S. PAHs sorption and desorption on soil influenced by pine needle litter-derived dissolved organic matter. *Pedosphere* **2014**, *24*, 575–584. [[CrossRef](#)]
150. He, Y.; Liu, C.; Tang, X.-Y.; Xian, Q.-S.; Zhang, J.-Q.; Guan, Z. Biochar impacts on sorption-desorption of oxytetracycline and florfenicol in an alkaline farmland soil as affected by field ageing. *Sci. Total Environ.* **2019**, *671*, 110–119. [[CrossRef](#)]
151. Kah, M.; Sigmund, G.; Chavez, P.L.M.; Bielská, L.; Hofmann, T. Sorption to soil, biochar and compost: Is prediction to multicomponent mixtures possible based on single sorbent measurements? *PeerJ* **2018**, *6*, e4996. [[CrossRef](#)]
152. Shang, X.; Wu, S.; Liu, Y.; Zhang, K.; Guo, M.; Zhou, Y.; Zhu, J.; Li, X.; Miao, R. Rice husk and its derived biochar assist phytoremediation of heavy metals and PAHs co-contaminated soils but differently affect bacterial community. *J. Hazard. Mater.* **2024**, *467*, 133684. [[CrossRef](#)]
153. Zhang, X.; Gong, Z.; Allinson, G.; Li, X.; Jia, C. Joint effects of bacterium and biochar in remediation of antibiotic-heavy metal contaminated soil and responses of resistance gene and microbial community. *Chemosphere* **2022**, *299*, 134333. [[CrossRef](#)]
154. Nguyen, T.B.; Sherpa, K.; Bui, X.T.; Nguyen, V.T.; Vo, T.D.H.; Ho, H.T.T.; Chen, C.W.; Dong, C.D. Biochar for Soil Remediation: A Comprehensive Review of Current Research on Pollutant Removal. *Environ. Pollut.* **2023**, *337*, 122571. [[CrossRef](#)]
155. Castaldi, S.; Rioldino, M.; Baronti, S.; Esposito, F.R.; Marzaioli, R.; Rutigliano, F.A.; Vaccari, F.P.; Miglietta, F. Impact of Biochar Application to a Mediterranean Wheat Crop on Soil Microbial Activity and Greenhouse Gas Fluxes. *Chemosphere* **2011**, *85*, 1464–1471. [[CrossRef](#)]
156. Zheng, Y.; Wan, Y.; James, J.; Devereux, R.; Noerpel, M.; Wei, J.; Zhang, Y.; Yang, Y.; Huang, J.; Chen, H.; et al. Remediation of Pb Contaminated Soil with Recovered Pladen Engineered Biochar: Effects on Pb Speciation and Soil Microbial Community. *Chem. Eng. J.* **2026**, *532*, 174220. [[CrossRef](#)]
157. Sui, F.; Wang, J.; Zuo, J.; Joseph, S.; Munroe, P.; Drosos, M.; Li, L.; Pan, G. Effect of Amendment of Biochar Supplemented with Si on Cd Mobility and Rice Uptake over Three Rice Growing Seasons in an Acidic Cd-Tainted Paddy from Central South China. *Sci. Total Environ.* **2020**, *709*, 136101. [[CrossRef](#)]
158. Stefaniuk, M.; Tsang, D.C.W.; Ok, Y.S.; Oleszczuk, P. A field study of bioavailable polycyclic aromatic hydrocarbons (PAHs) in sewage sludge and biochar amended soils. *J. Hazard. Mater.* **2018**, *349*, 27–34. [[CrossRef](#)]
159. Mazzurco-Miritana, V.; Passatore, L.; Zacchini, M.; Pietrini, F.; Peruzzi, E.; Carloni, S.; Rolando, L.; Garbini, G.L.; Caracciolo, A.B.; Silvani, V.; et al. Promoting the remediation of contaminated soils using biochar in combination with bioaugmentation and phytoremediation techniques. *Sci. Rep.* **2025**, *15*, 11231. [[CrossRef](#)]
160. Duan, Z.; Chen, C.; Ni, C.; Xiong, J.; Wang, Z.; Cai, J.; Tan, W. How Different Is the Remediation Effect of Biochar for Cadmium Contaminated Soil in Various Cropping Systems? A Global Meta-Analysis. *J. Hazard. Mater.* **2023**, *448*, 130939. [[CrossRef](#)]
161. Lima, J.Z.; Rodrigues, V.G.S. Effects of Biochar on Soil Contaminated by Metals and Metalloids from Slag Disposal of an Old Environmental Liability in Ribeira Valley, Brazil. *J. Environ. Manag.* **2025**, *373*, 123782. [[CrossRef](#)]
162. Spokas, K.A.; Baker, J.M.; Reicosky, D.C. Ethylene: Potential Key for Biochar Amendment Impacts. *Plant Soil* **2010**, *333*, 443–452. [[CrossRef](#)]
163. Dudnikova, T.; Wong, M.H.; Minkina, T.; Sushkova, S.; Bauer, T.; Khroniuk, O.; Barbashev, A.; Shuvaev, E.; Nemtseva, A.; Kravchenko, E. Effects of Pyrolysis Conditions on Sewage Sludge-Biochar Properties and Potential Risks Based on PAH Contents. *Environ. Res.* **2025**, *266*, 120444. [[CrossRef](#)]
164. Syguła, E.; Piasecka, K.; Łyczko, J.; Białowiec, A. The Potential of Decision Tree Application in Threshold Analysis of Hazardous Volatile Organic Compound Release from Biochar: Implications for Environmental Risk Assessment. *Sci. Total Environ.* **2025**, *998*, 180252. [[CrossRef](#)]
165. Haelderms, T.; Campion, L.; Kuppens, T.; Vanreppelen, K.; Cuypers, A.; Schreurs, S. A Comparative Techno-Economic Assessment of Biochar Production from Different Residue Streams Using Conventional and Microwave Pyrolysis. *Bioresour. Technol.* **2020**, *318*, 124083. [[CrossRef](#)]
166. Liao, W.; Zhang, X.; Yang, R.; Yang, H.; Wang, J.; Zhang, S.; Chen, H. Biochar Structure Regulation Based on the Evaluation of Adsorption Efficiency, Anti-Aging Ability and Economy during Soil Heavy Metal Remediation. *J. Anal. Appl. Pyrolysis* **2025**, *191*, 107223. [[CrossRef](#)]

**Disclaimer/Publisher's Note:** The statements, opinions and data contained in all publications are solely those of the individual author(s) and contributor(s) and not of MDPI and/or the editor(s). MDPI and/or the editor(s) disclaim responsibility for any injury to people or property resulting from any ideas, methods, instructions or products referred to in the content.